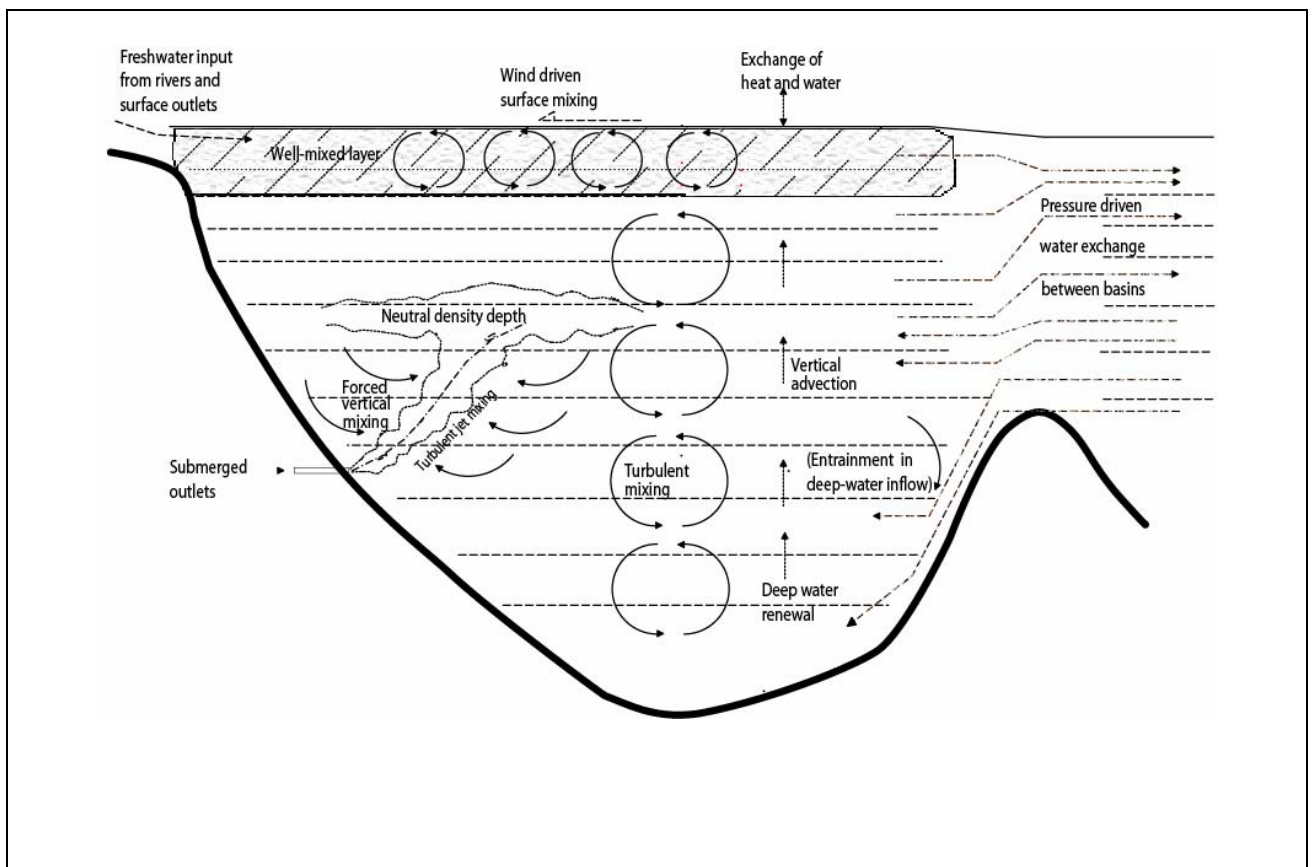


# Critical loads for nitrogen in fjords; evaluation of effects of nitrogen leaching from explosives used for E18 road construction in Aust-Agder



Main Office	Regional Office, Sørlandet	Regional Office, Østlandet	Regional Office, Vestlandet	Regional Office, Midt-Norge
Gaustadalléen 21 N-0349 Oslo, Norway Phone (47) 22 18 51 00 Telefax (47) 22 18 52 00 Internet: www.niva.no	Televeien 3 N-4879 Grimstad, Norway Phone (47) 37 29 50 55 Telefax (47) 37 04 45 13	Sandvikaveien 41 N-2312 Ottestad, Norway Phone (47) 62 57 64 00 Telefax (47) 62 57 66 53	P.O.Box 2026 N-5817 Bergen, Norway Phone (47) 55 30 22 50 Telefax (47) 55 30 22 51	P.O.Box 1266 N-7462 Trondheim Phone (47) 73546385 Telefax (47) 73546387

Title Critical loads for nitrogen in fjords; evaluation of effects of nitrogen leaching from explosives used for E18 road construction in Aust-Agder.	Serial No. 5470-2007	Date July 30, 2007
	Report No. Sub-No. O-27171	Pages Price 38
Author(s) Atle Hindar, Birger Bjerkeng, Torulv Tjomsland and Torbjørn Johnsen	Topic group Eutrophication	Distribution
	Geographical area Aust-Agder	Printed NIVA

Client(s) CJV E18 Grimstad-Kristiansand	Client ref. Letter of March 8, 2007
--	--

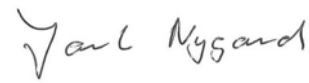
**Abstract**

The new road, E18, between Grimstad and Kristiansand in Aust-Agder county, will be constructed by blasting of about 15.9 mill. tons (7.7 mill m<sup>3</sup>) of rock. This will be carried out by use of 0.65 or 2.5 kg explosives per m<sup>3</sup> rock for earth works and tunnel works, respectively, and potentially (if 100 % leaching) result in runoff of 900 tons of nitrogen. Potentially about 500 tons of N will enter the more or less landlocked fjords Kaldvellfjorden, Vallesverdfjorden and Isefjærfjorden. We have compared this loading with background and other man-made N-loads by use of the river transport model TEOTIL. Further, we calibrated and run the NIVA fjord model to estimate the change in concentrations of nitrogen, particulate matter and the oxygen regime in these three fjords. Nitrate concentrations are estimated to potentially increase by a factor of 2 for 2 years at most. The results are discussed on basis of relative increase in nitrate and the impact on algae growth and composition. Due to the dilution by sea water, the general phosphorus limitation in the fjords and grazing by zooplankton, biological effects and effects on the oxygen regime in the fjords are estimated to be minor. If we also assume that the actual N-leaching will be far less than the potential, we are relatively certain that the effects will be insignificant.

4 keywords, Norwegian 1. Vegarbeid 2. Fjorder 3. Nitrogen 4. Kritisk belastning	4 keywords, English 1. Road construction 2. Fjords 3. Nitrogen 4. Critical Load
---	---

  
 Atle Hindar  
 Project manager

  
 Brit Lisa Skjelkvåle Monsen  
 Research manager

  
 Jarle Nygard  
 Strategy Director

**Critical loads for nitrogen in fjords; evaluation of effects of nitrogen leaching from explosives used for E18 road construction in Aust-Agder**

## Preface

According to the discharge permit for new E18 Grimstad-Kristiansand accept limits for nitrogen shall not be exceeded. These limits were set in brooks, rivers and lakes partly to protect the land-locked fjords from increased N input.

At a meeting with Fylkesmannen, Statens vegvesen, Agder OPS vegselskap, CJV and NIVA on January 31, 2007, a critical load concept for N to fjords was discussed. NIVA was encouraged to propose a project on this basis, and after acceptance of the idea by Fylkesmannen, the offer from NIVA was accepted by CJV.

After delimitation of catchment/fjord areas and sectioning of the road, CJV calculated amount of blasted rock from the road-construction for these sections. CJV also gave numbers for the use of explosives. These numbers were used by NIVA to calculate the potential increase in N input to the fjords.

Contact person at CJV has been Dr. Martin Schreck.

Grimstad, July 30, 2007

*Atle Hindar*

---

# Contents

<b>1. Introduction</b>	<b>5</b>
<b>2. Methods</b>	<b>5</b>
<b>3. Delimitation of catchments</b>	<b>6</b>
<b>4. Calculation of P and N loads to fjords by use of the TEOTIL-model</b>	<b>9</b>
<b>5. Hydrochemical observations in fjords</b>	<b>11</b>
<b>6. Simulation of effects with the NIVA fjord model</b>	<b>12</b>
6.1 General description of the model	12
6.2 Basin subdivision and topography in model setup	14
6.3 Input data used in model simulations	16
6.3.1 Water level variations on outer boundary	16
6.3.2 Hydrochemical conditions on outer boundary	17
6.3.3 Meteorological input data	18
6.3.4 Ordinary runoff to the fjord areas	18
6.3.5 Nitrogen runoff from explosives used in road construction	20
6.4 Scenarios with N from the road construction – comparison with background scenarios.	23
<b>7. Discussion</b>	<b>29</b>
<b>8. Conclusion</b>	<b>30</b>
<b>9. References</b>	<b>30</b>
<b>Appendix A. Hydrochemical boundary conditions - monthly statistics</b>	<b>31</b>
<b>Appendix B. Simulation results for background scenario</b>	<b>34</b>

# 1. Introduction

Several hundred tons of nitrogen (N) from explosives will be released as part of the construction work along the new E18 Grimstad - Kristiansand. Some of this N will leach as nitrate to freshwater systems and to the fjords along the line. This will increase the concentrations in freshwater recipients, as already documented by the environmental monitoring program (MKP; Miljøkontrollprogrammet) for this project, and probably also in the fjords.

Nitrogen is generally not believed to regulate algae growth in freshwaters, as phosphorus (P) is the main growth-limiting substance. Cases of the contrary may be found, however, and data from the MKP suggest that N is depleted during summertime in the small lake Lomtjenn downstream one of the large deposits for sulphide-containing bedrock. Increased N may therefore stimulate algae production in this single lake if sufficient P is available.

As long as pH is lower than 8, nitrogen is thus not expected to significantly affect freshwaters. Above pH 8 an increasing part of the reduced forms of N ( $\text{NH}_4^+ + \text{NH}_3$ ) will occur as ammonia ( $\text{NH}_3$ ), which is toxic to fish at low concentrations. If pH is kept below 8, problems with ammonia are avoided.

In fjords the growth limiting factors may be different from freshwaters, as both nitrate and silicate may be limiting in periods of reduced availability and sufficient P supply. An increase in nitrate concentrations may therefore result in increased algal growth.

Due to anticipated effects in freshwaters and fjords, Statens vegvesen had to apply for a discharge permit for the E18 Grimstad-Kristiansand. The discharge permit given by Fylkesmannen in the two Agder counties sets limits for several water chemistry components. Accept limits for N were partly for the protection of the marine fjords. No calculations of the potential N load and critical loads (CL) for the fjords existed, however. That is why restrictions were set only for streams and lakes. The CL principle is based on established dose-response relationships. According to this principle a certain increase in loading, although significant, may not necessarily be regarded as harmful. In order to suggest targets for N that is more closely linked to CL and the fjords themselves, this project was initiated.

The main objective of the work was to obtain a basis for a switch from the present accept limits for N (nitrate+total ammonium) in the discharge permit to acceptable N-loads for fjords. This was done by:

- devide single land/fjord catchments from each other as a basis for a sectioning of the road line+deposits,
- estimate the potential and expected N load to the respective fjords and areas of open sea over a course of five years (CJV calculated the N production in these sections until end of 2011),
- compare this load with known N-sources,
- set up a fjord model for three fjords to calculate change in concentrations and evaluate effects, and
- give advise on critical loads for the extra N input.

# 2. Methods

To evaluate the effects on fjords of nitrogen loading from explosives, we compared this added N-loading with other sources on land and in the fjords themselves. Two existing models were used for this purpose.

The river model TEOTIL was well suited for the first part. It uses statistical data from all known sources on land on a subcatchments scale, both natural and man-made. Loading from areas were calculated on a monthly basis by use of specific coefficients for each particular area type and by distributing the loads according to monthly runoff characteristics. Loading from point sources were distributed evenly throughout the year.

The NIVA fjord model was calibrated on basis of measured water chemistry in the fjords, together with oceanographic and topographic characteristics. The potential increase in nitrate-concentrations due to the added loading was modelled by running the calibrated model with the added loading.

The potential increase in nitrate concentrations was evaluated based on the magnitude of the difference, concentrations of other nutrients, algae dynamics and knowledge on how a fjord ecosystem may handle the N-increase.

The models and their use are further described in later sections.

### 3. Delimitation of catchments

NVE Atlas (see Atlas at [www.nve.no](http://www.nve.no)) was used for delimitation of the catchments. We identified six sections (**Figure 1-Figure 2**) of the road-construction draining to vulnerable fjords along the coast. The vulnerable (1-6) and other (0) sections are suggested in **Table 1**:

**Table 1.** Vulnerable fjords/road-sections (1-6) and other parts of the coast (0) from east (Grimstad) to west (Kristiansand).

Fjord area	Characteristics/Vulnerability
0. East to Morvigfjorden	Open sea
0. Morvigkilen	Narrow fjord to open sea, no threshold. Camping ground
1. Reddalskanalen/Strandfjorden	Tide current and open sea, P load from agriculture upstream
0. Nørholmkilen, Bufjorden	Narrow fjord to open sea
2. Kaldvellfjorden	Land-locked, low P load, insignificant retention in soils and water
3. Tingsakerfjorden/Skallefjorden	Fjord more open, valuable eelgras habitats, high P load from Lillesand. Some retention/dilution of N in Lake Glamslandsvann. Retention in deep soils in the Moelva valley along the road line
4. Vallesverdfjorden	Land-locked, low P load, retention/dilution of N in the lakes Urdevann, Kviksvann, Kråkevann and Beintjenn
5. Isefjærfjorden	Land-locked, low P load, retention/dilution of N in Lake Studevann
0. Topdalsfjorden (to the west)	Runoff in the Krogevatn/Grasvatn to Topdalsfjorden and then open sea. Retention/dilution of N in the lakes
6. Innermost part of Kvåsefjorden	Land-locked, P load from Dyreparken++. Retention/dilution of N in ponds/small lakes down the Åna River
0. Topdalsfjorden	Open sea + retention/dilution in lakes Drangsvatna

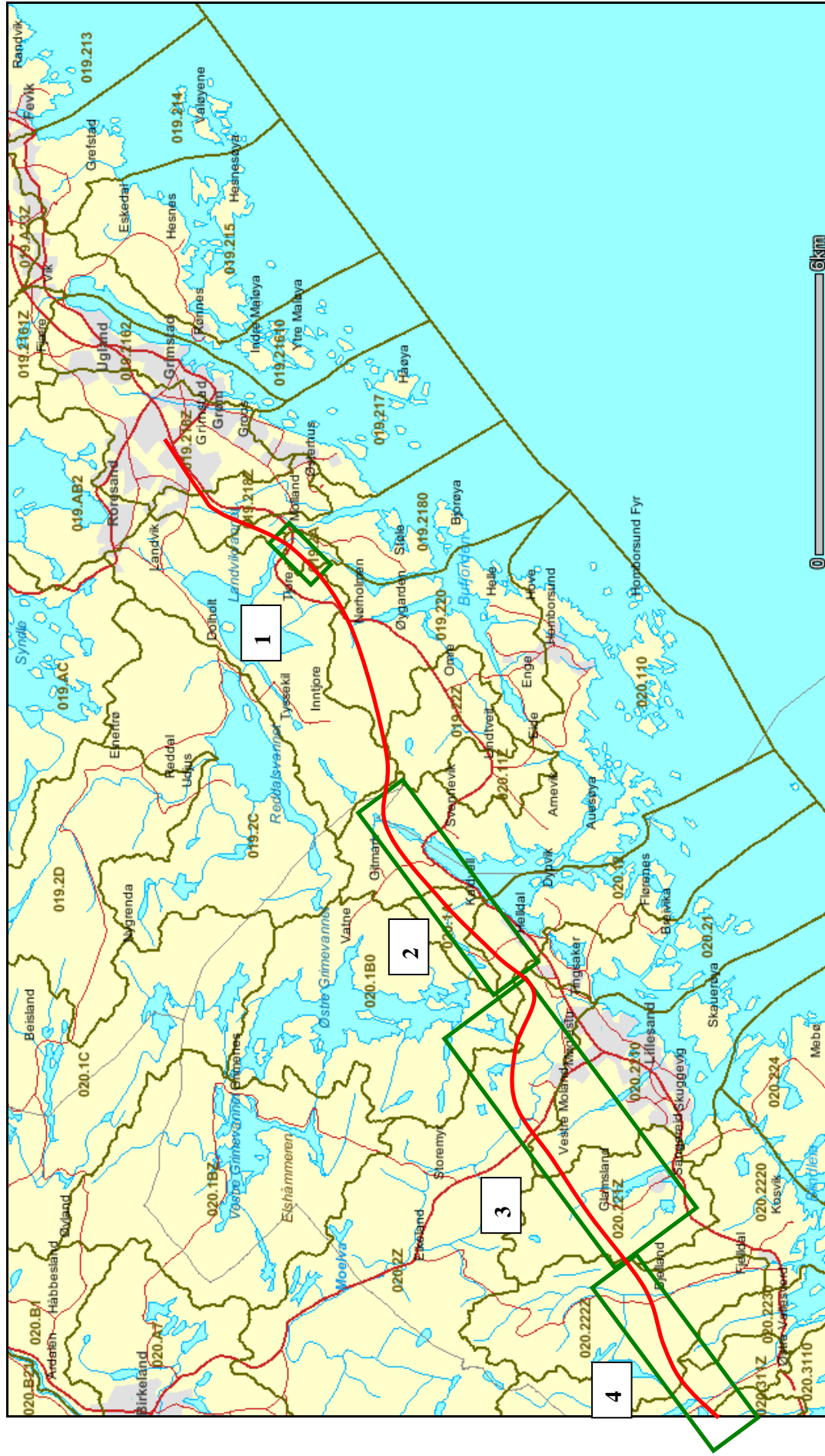


Figure 1. New E18 east with sections 1 Reddalskanalen, 2 Kaldvellfjorden, 3 Tingsakerfjorden+Skallefjorden and part of 4 Vallesverdfjorden.





## 4. Calculation of P and N loads to fjords by use of the TEOTIL-model

The background loads (natural and man-made, except new E18) were calculated by the model TEOTIL, (Selvik et al., 2005; Tjomsland and Bratli, 1996). TEOTIL utilises statistical data (usually on an annual basis) on discharges from point sources (waste water treatment plants and industries), information about the degree of connection to municipal sewage network, type specific (forest, mountain, agricultural land and lake) area run-off coefficients (export coefficients) and the actual water flow. No processes are represented in the land-phase of the model. In order to calculate the retention of nutrients in the water bodies, TEOTIL requires information about the structure of the river system (sub-catchments, rivers and lakes). The model used the NVE's Regine sub-catchment system as minimum computation elements.

The point sources and area-specific coefficients represent 2005. The water-flows are mean values from the period 1960-1990 according to the specific runoff for each sub-catchment (NVE, Regine).

Areas of land cover (forest, mountain, agriculture and lakes) for each Regine sub-catchments were found from digital maps by use of GIS, Arcview. Data from sewage were localized from coordinates. Loads from scattered population only existed as a sum for each municipality. In the model these loads were uniformly spread over the whole area of the municipality. The drainage areas to the fjords are shown in **Figure 3**, and data for areas and mean water-flow are given in **Table 2** and **Table 3**.

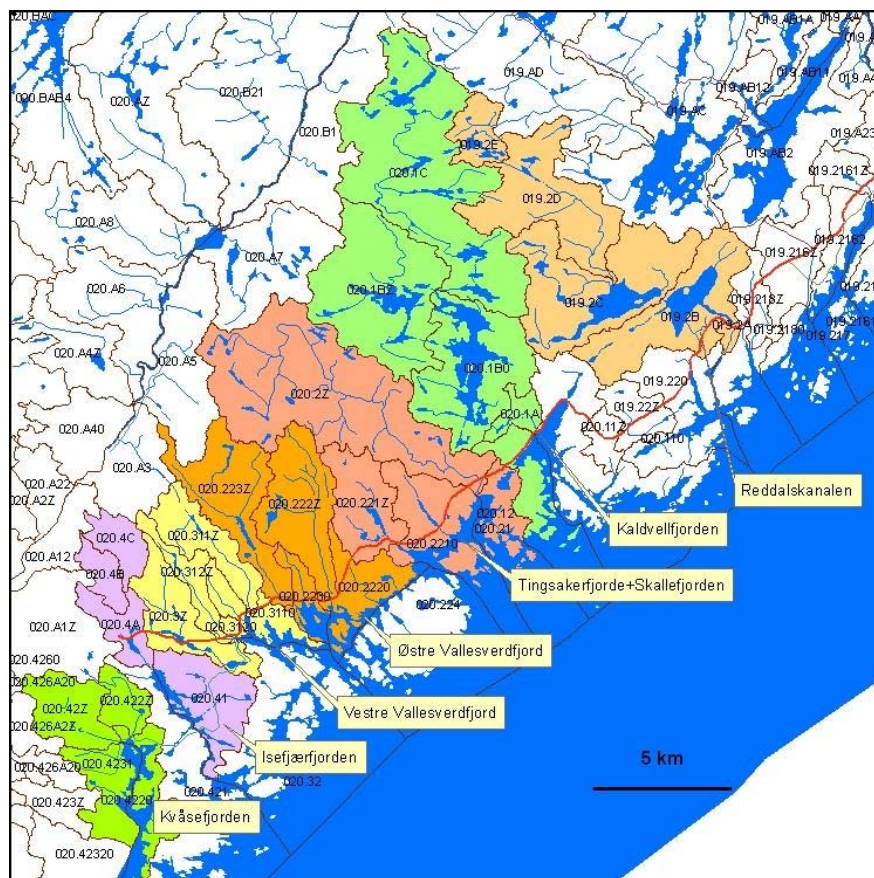


**Figure 3.** Drainage areas (Regine sub-cathments) with runoff to vulnerable fjords.

The calculated annual loads are also given on a monthly basis. Loads from municipal sources were divided by twelve, whereas losses from areas are proportional to the monthly water flow. The total P and N loads to the fjords are given in **Table 4** and **Table 5**. The P loads are in the range 0.15-0.65 tons per year, and the N loads are 5-44 tons per year.

**Table 2.** Background data for the Regine drainage areas for different fjord regions

Land cover	Area	Forest	Mountain	Lake	Agriculture
Fjord	Regine	km <sup>2</sup>	km <sup>2</sup>	km <sup>2</sup>	km <sup>2</sup>
1.Reddalskanalen	019.2A	53.790	45.176	1.615	2.772
2.Kaldvellfjorden_vest	020.12	79.057	68.776	2.746	1.293
3.Tingsakerfj.+Skallefj.	020.21	20.222	12.655	0.304	7.263
4a.Vallesverdfjorden_øst	020.2230	31.788	29.633	2.155	0
4b.Vallesverdfjorden_vest	020.3110	23.234	14.351	8.883	0
5.Isefjærfjorden	020.41	18.402	14.88	2.068	0.872
6.Kvåsefjorden	020.4220	18.332	12.906	4.902	0

**Table 3.** Mean water flow 1960-1990 to different fjord regions

Mean water flow 1960-1990	Year	Jan	Feb	Mar	Apr	Mai	Jun	Jul	Aug	Sep	Okt	Nov	Des
Location	m <sup>3</sup> /s												
1.Reddalskanalen	1.532	1.476	1.272	0.972	1.752	2.652	1.752	1.248	0.996	1.236	1.728	1.932	1.356
2.Kaldvellfjorden_vest	2.360	2.820	2.412	1.908	3.000	3.000	1.848	1.488	1.320	1.896	2.772	3.348	2.496
3.Tingsakerfj.+Skallefj.	0.411	0.492	0.420	0.336	0.516	0.528	0.324	0.264	0.228	0.324	0.480	0.588	0.432
4a.Vallesverdfjorden_east	0.884	1.056	0.900	0.720	1.128	1.128	0.696	0.552	0.492	0.708	1.044	1.260	0.936
4b.Vallesverdfjorden_vest	0.628	0.756	0.648	0.504	0.804	0.804	0.492	0.396	0.348	0.504	0.744	0.888	0.660
5.Isefjærfjorden	0.465	0.552	0.480	0.372	0.588	0.588	0.360	0.288	0.264	0.372	0.552	0.660	0.492
6.Kvåsefjorden	0.401	0.480	0.408	0.324	0.504	0.516	0.312	0.252	0.228	0.324	0.468	0.576	0.420

**Table 4.** Phosphorus load to different fjord regions

Phosphorus load 2005	Year	Jan	Feb	Mar	Apr	Mai	Jun	Jul	Aug	Sep	Okt	Nov	Des
Location	(ton P)												
1.Reddalskanalen	0.352	0.029	0.026	0.022	0.032	0.045	0.032	0.026	0.022	0.025	0.032	0.035	0.027
2.Kaldvellfjorden_vest	0.576	0.054	0.049	0.042	0.057	0.057	0.041	0.036	0.034	0.042	0.054	0.062	0.050
3.Tingsakerfj.+Skallefj.	0.654	0.061	0.055	0.048	0.064	0.064	0.047	0.041	0.039	0.047	0.061	0.070	0.057
4a.Vallesverdfjorden_øst	0.229	0.021	0.019	0.017	0.022	0.022	0.017	0.016	0.015	0.017	0.021	0.023	0.020
4b.Vallesverdfjorden_vest	0.192	0.017	0.016	0.015	0.018	0.018	0.015	0.014	0.013	0.015	0.017	0.019	0.016
5.Isefjærfjorden	0.223	0.020	0.019	0.017	0.021	0.021	0.016	0.015	0.014	0.016	0.020	0.023	0.019
6.Kvåsefjorden	0.150	0.013	0.013	0.012	0.014	0.014	0.012	0.011	0.011	0.012	0.013	0.014	0.013

**Table 5.** Nitrogen load to different fjord regions

Nitrogen load 2005	Year	Jan	Feb	Mar	Apr	Mai	Jun	Jul	Aug	Sep	Okt	Nov	Des
Location	(ton N)												
1.Reddalskanalen	25.414	2.040	1.771	1.389	2.408	3.580	2.412	1.753	1.421	1.739	2.381	2.637	1.884
2.Kaldvellfjorden_vest	37.287	3.647	3.167	2.573	3.861	3.871	2.509	2.075	1.876	2.557	3.598	4.281	3.270
3.Tingsakerfj.+Skallefj.	44.391	4.022	3.735	3.380	4.150	4.156	3.342	3.082	2.963	3.370	3.993	4.402	3.797
4a.Vallesverdfjorden_øst	12.346	1.206	1.049	0.854	1.276	1.279	0.833	0.691	0.626	0.848	1.190	1.414	1.082
4b.Vallesverdfjorden_vest	9.205	0.882	0.780	0.653	0.928	0.930	0.639	0.546	0.503	0.649	0.872	1.018	0.802
5.Isefjærfjorden	9.538	0.919	0.808	0.672	0.968	0.970	0.657	0.557	0.511	0.668	0.908	1.065	0.832
6.Kvåsefjorden	5.689	0.548	0.482	0.401	0.577	0.579	0.392	0.333	0.306	0.399	0.541	0.635	0.496

The potential added N-loads from explosives are significant when compared with annual figures for natural and the pre-blasting man-made contributions (**Table 6**). For the three fjords we have chosen for modelling, the potential added N-loads for Kaldvellfjorden and Isefjærfjorden are 3-5 times the annual background, whereas the load for Vallesverdfjorden is more than 15 times the annual background. The three other fjords are within this range.

**Table 6.** Nitrogen loads from background sources (annual; natural and agricultural mainly) and the total added loads from explosives used for the E18 road construction.

	Background Tons N/year	E18 Total tons N
1.Reddalskanalen	25.4	49.2
2.Kaldvellfjorden	37.3	176.5
3.Tingsakerfj.+Skallefj.	44.4	174.7
4.Vallesverdfjorden	21.6	336.5
5.Isefjærfjorden	9.5	25.6
6.Kvåsefjorden	5.7	13.9

## 5. Hydrochemical observations in fjords

Hydrographic and hydrochemical data from March 2006 through March 2007 form a background for adjusting and calibrating the fjord model and assessing the effects of nitrogen additions. In this section we refer to monitoring stations of the environmental monitoring program for the E18 construction work (see Kroglund et al. 2007 for station numbers). The stations are named K1-K4 in Kaldvellfjorden, V1-V4 in Vallesverdfjorden and I1-I2 in Isefjærfjorden.

The surface layer in the fjords, from 2 to 10 m thickness, had salinities in spring and summer varying from 14 to 26 ‰ and from 18 to 26 ‰. In winter the surface salinity is normally within 23-30 ‰, but can be down to 18 ‰. Below 15 m the salinity is more or less constant at 32-33 ‰.

Oxygen concentrations in Kaldvellfjorden were often reduced below 5 m depth at the monitoring station K2, and at deeper depths than 15 m at K4. On 20 April 2006, oxygen had a minimum at 10 m depth, to <1 ml/l at K2 and 4 ml/l at K4, with high values (8 ml/l) both at the surface and below 14 m. This coincided with high salinities up to 3 m depth, probably a result of old, oxygen-depleted deep-water being lifted as a result of deep water renewal with oxygen-rich denser water from the outside. In May and June this minimum had gone, but oxygen concentrations were gradually reduced in the deeper layers, to <1 ml/l at 25 m in August at K4. During winter 2006-2007 the oxygen conditions improved again at K4, but still with low values at K2.

In Vallesverdfjord, oxygen conditions were generally good in the eastern basin (station V2) down to 40 m depth, with all concentrations above 8 mg/l. In the innermost, western basin (station V4) there were reduced oxygen concentrations below 10-15 m depth, to less than 1 mg/l at 30 m during 2006. In March 2007 new oxygen-rich water had renewed the deeper layers at V2 and brought the oxygen concentrations up to 7 mg/l.

Isefjærfjord had oxygen depletion below 10 m depth in the innermost basin. Hydrogen sulphide was measured twice at station I1; at 25 m depth on 20 April and at 15 m depth on 20 June. Oxygen sensor data show concentrations <0.5 ml/l at 20 m depth in most observations, but the sensor will not show hydrogen sulphide. In December 2006 oxygen was low through most of the water column, with a minimum of 1.5 ml/l at 2-3 m depth, in water with particularly high salinities. This was also apparently a result of deep-water renewal with old water being lifted towards the surface.

Nutrient and particle concentrations had more or less the same development in all fjords in the upper 10 m.

Total phosphorus in the surface layer (1 m depth) stayed at 7-10  $\mu\text{g P/l}$  in the surface from late winter and through summer, increased to 20-25 some time between August and December 2006, and then dropping again to 7-11  $\mu\text{g P/l}$  in late March 2007. In summer the phosphorus concentrations were fairly homogeneous down to 5 - 10 m depth; in winter there is a gradient with values increasing from 20-25  $\mu\text{g P/l}$  in the surface to 40  $\mu\text{g P/l}$  at 10 m depth. Orthophosphate was measured to be from 40 to 10 % of total phosphorus from 13 March to 16 June 2006, with the rest probably bound in biomass; after that orthophosphate was not measured.

In Kaldvellfjord, station K4, surface concentrations of total suspended matter (TSM) varies between 0.3 and 0.5 mg/l from March to August 2008, indicating at most 150-200  $\mu\text{g}$  particulate organic carbon (if carbon is assumed to make up 40 % of total dry matter). With normal N:C ratios for organic matter, this should indicate that at most 15-20  $\mu\text{g N/l}$  is bound in phytoplankton in late winter.

Total phosphorus had low values in summer, about 7-10  $\mu\text{g P/l}$ , with increasing concentrations from summer to winter below the surface layer, to about 35-40  $\mu\text{g P/l}$  in January 2007. On 21 March, concentrations were reduced to 7-10  $\mu\text{g P/l}$  from the surface down to 7 m depth, through the whole stratified layer. Orthophosphate, only measured in the surface layer and only during winter and spring 2006, varies between 1 and 5  $\mu\text{g/l}$ .

Nitrate is totally depleted in Kaldvellfjord in July and August 2006 in the upper 10 m, and concentrations were 140-180  $\mu\text{g N/l}$  from the surface to 10 m in winter 2007. The concentrations drop to below 10  $\mu\text{g N/l}$  in March 2007, between 3 and 7 m at K2 and from 3 and 5 m at K4, with higher values remaining at the surface and at 10 m depth. Total nitrogen was only measured in the surface, and only during winter and spring 2006, not coinciding with nitrate measurements. The concentration varied from 200 to 400  $\mu\text{g totN/l}$  in winter, and was 150  $\mu\text{g totN/l}$  in March 2006. *Since in the model inactive nitrogen of up to 100  $\mu\text{g N/l}$  is thought to come in addition to the model concentrations in the fjord, this should correspond to model concentrations of 100-300  $\mu\text{g/l}$  in winter, down to 50  $\mu\text{g N/l}$  in March.*

## 6. Simulation of effects with the NIVA fjord model

### 6.1 General description of the model

The NIVA fjord model describes eutrophication response to nutrient and organic matter loading through simulation of primary production, sinking and degradation of organic matter. The model structure and the first application of it is described by Bjerkeng (1994 a,b).

The chemical/biological processes are simulated in a physical framework with the fjord divided in a variable number of basins, each basin divided vertically in a variable number of layers. The model is driven by data for land runoff, weather and conditions on the outer boundary as functions of time.

**Figure 4** shows the main physical processes included in the model description, illustrated for one basin. Vertical mixing within each basin and horizontal transports between basins are dynamically coupled to the density field within each basin and to the difference in density fields of interconnected basins. Empirical relations between mixing and vertical stratification are used to describe vertical mixing.

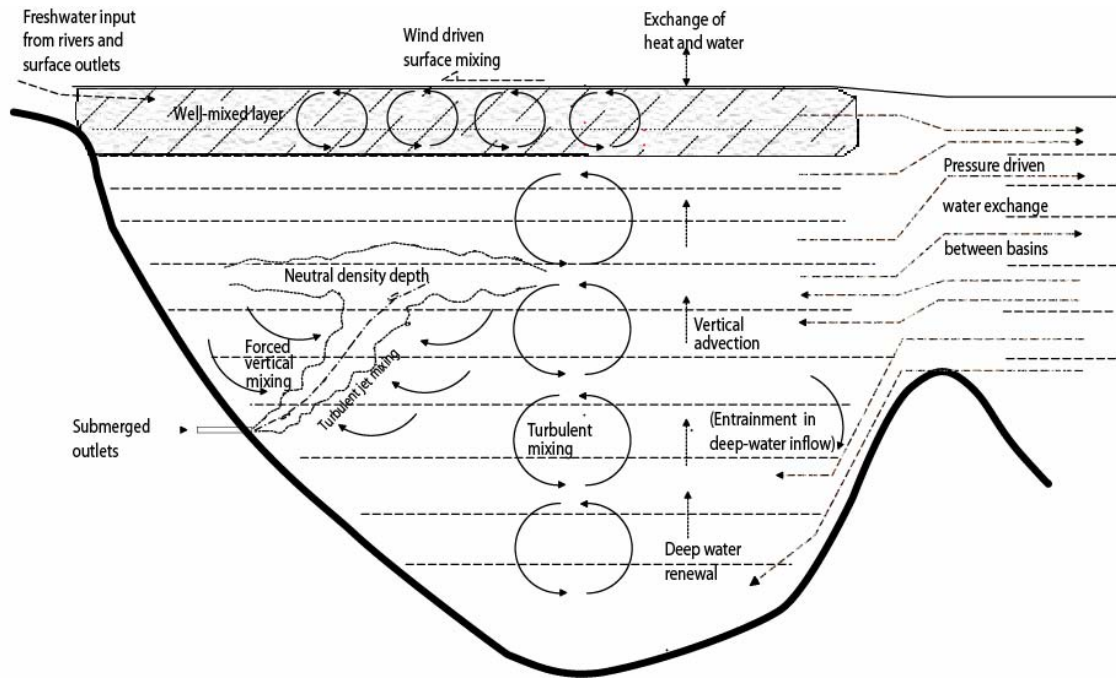


**Figure 4.** Physical processes within each basin, as used in the NIVA fjord model.

The biological submodel for the water column and benthos describes primary production by phytoplankton, divided in two groups with different characteristics (loosely characterized as diatoms and flagellates), grazing by zooplankton and mussels. Primary production is considered to be a function of light, temperature, available nitrogen and phosphorus and for diatoms also silicon. Diurnal variations are included. The model also includes excretion of DOC and bacterial growth connected to DOC. Particle sinking and degradation in water and sediment under different oxygen regimes including denitrification are described by dynamic sub-models. **Figure 5** shows the main biochemical structure of the model.

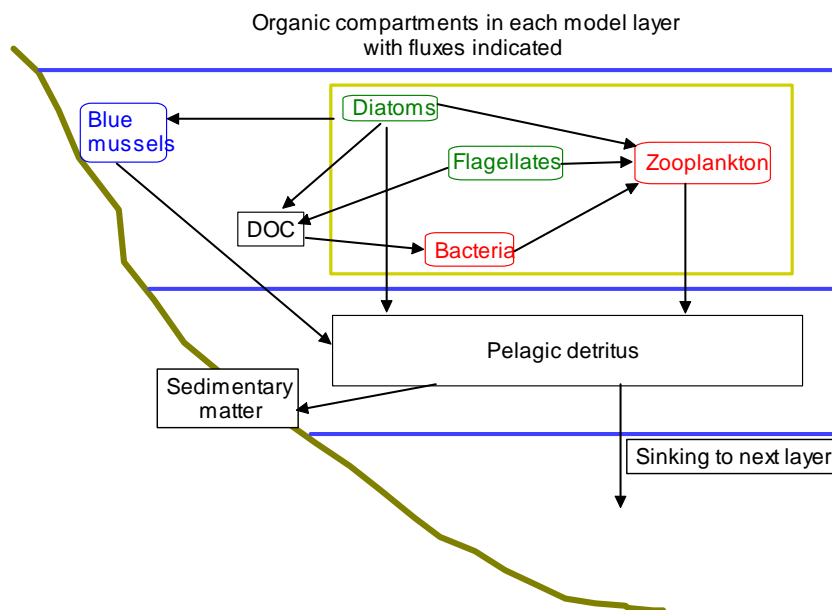


**Figure 5.** Biochemical components within each layer, as used in the NIVA fjord model

## 6.2 Basin subdivision and topography in model setup

Kaldvellfjord has been divided in 6 basins as shown in the map in **Figure 6**, with the inner part that receives nitrogen from the E18 project divided in two basins, the north-eastern part from Kilen to Kaldvell and the southwestern main basin in the region Kaldvell-Helldal-Dypvik. Ordinary runoff is also distributed to these two basins in the model runs. The other 4 basins are transition areas towards the open coastal water.

Vallesverdfjord has been divided in 13 basins altogether, as shown in the map in **Figure 7**, two inner main basins that receives nitrogen from explosives, and 11 other basins. The ordinary runoff is distributed on the various basins as described in section 6.3.4.

Isefjærfjord is divided in 8 basins as shown in the map in **Figure 8**, with the inner basin as recipient for nitrogen from the road project, and the ordinary runoff is distributed as described in section 6.3.4

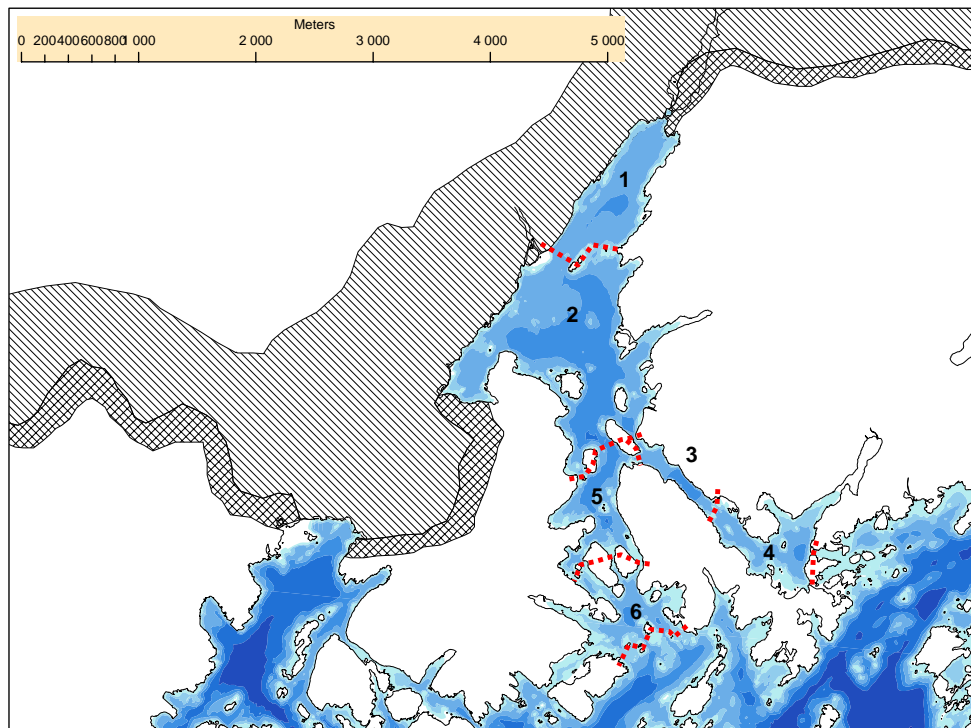


**Figure 6.** Kaldvellfjord, with basin subdivision (numbers 1-6) used in the model simulations. Basin boundaries are shown with red, dotted lines. Hatching marks the E18 project area.

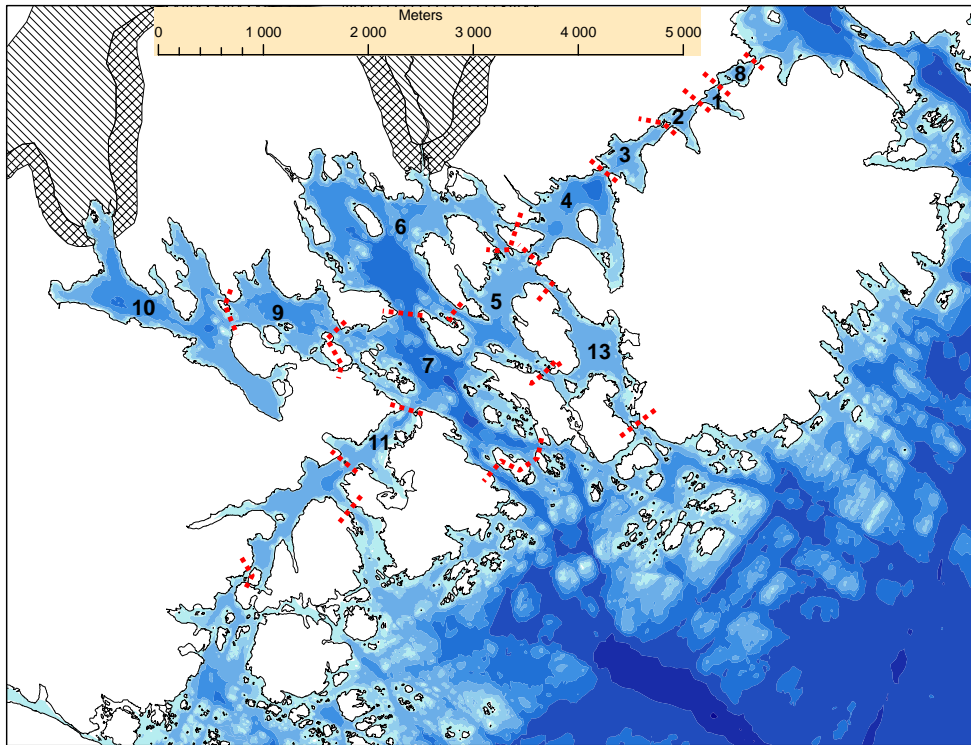


**Figure 7.** Vallesverdfjord, with basin subdivision (numbers 1-13) used in the model simulations. Basin boundaries are shown with red, dotted lines. Hatching marks the E18 project area.

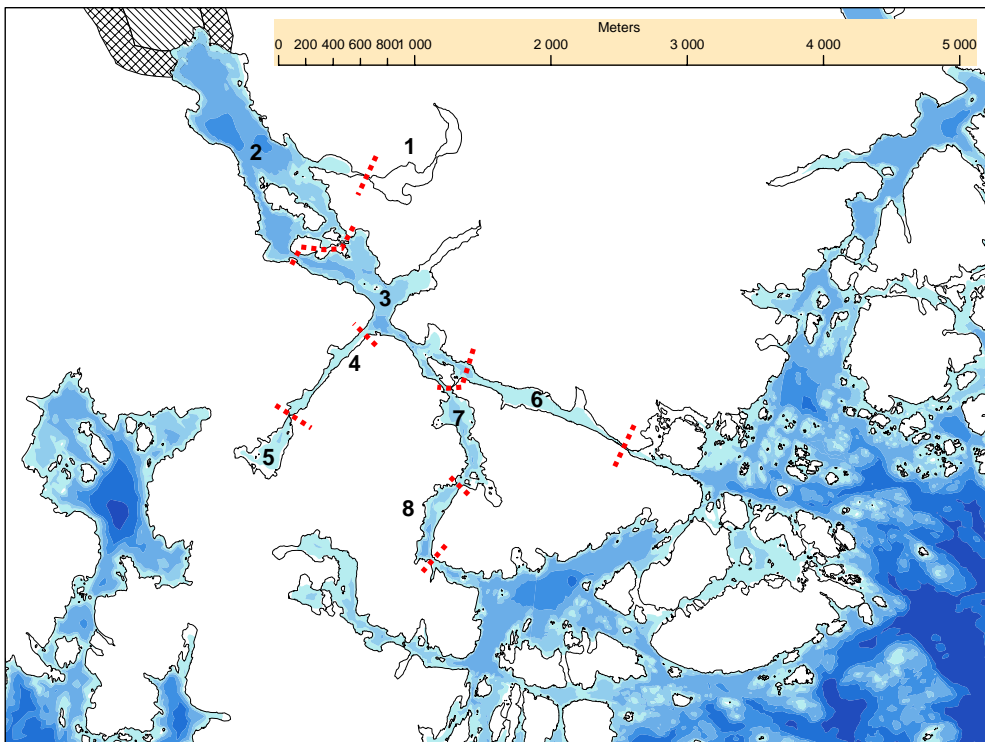


**Figure 8.** Isefjærfjord, with basin subdivision (numbers 1-8) used in the model simulations. Basin boundaries are shown with red, dotted lines. Hatching marks the E18 project area.



The topography description includes implementation of so called ‘buffer volumes’ between basins, representing water in the vicinity of the transport connections. The buffer volumes on each side represent water that has recently flowed across the connection, but has still not mixed into the main part of the receiving basin and may thus flow back unchanged with changed flow direction.

In the current model simulations buffer volume limits are defined based on an assessment of the topography, to represent intermediate volumes where it is likely that water may flow back and forth across the transport connection without being mixed into the main basin, but tuned to give realistic salinity differences in the inner basins, which are the main focus of the model simulations. The time constant has been set to 0.5 days, approximately one tidal period.

### 6.3 Input data used in model simulations

The model is driven by data for land runoff, weather and conditions on the outer boundary as functions of time. Historical time series are not available for runoff, so input data is generally created within the model simulations based on specifications as described below. For land runoff, monthly tables of N and P input calculated by the program TEOTIL is used (Selvik et al. 2005). The model creates time series with realistic variations around the seasonal curve described by the TEOTIL results. As for the weather, the available historical data sets from 1994-2003 at nearby Oksøy lighthouse has been used directly. Water level variations on the boundary are modelled based on harmonic tidal constants, and hydrochemical conditions on the outer boundary by a month-depth table of averages and standard deviations for the important variables involved in water quality description.

Thus, the simulations do not represent a specific period. The results should be seen as hypothetical scenarios, but with realistic seasonal and irregular variation patterns, including variation from year to year. The variations are created by random number sequences, built in such a way that different scenarios can be run with identical time series for input data for comparison of scenarios.

#### 6.3.1 Water level variations on outer boundary

The model requires water level variations on the outer boundary to be specified through tidal harmonic constants. Data on water level variations are available at <http://vannstand.statkart.no> with both harmonic constants and measured water level data, including the effect of weather. For the coastal area from Isefjærfjorden (N58°08', E8°15') to Kaldvellfjorden (N58°14', E8°27') the relevant measuring stations are Tregde, 6 km east of Mandal (N58°00', E07°34') and Helgeroa at Larvik (N59°00' N, E09°52'). **Table 7** lists the harmonic constants for the two stations.

**Table 7.** Harmonic constants for tidal water level variation, Mandal and Helgeroa.

	Tregde, 6 km east of Mandal			Helgeroa, Larvik		
Harmonic constants, as amplitude (cm)	SA	9.0	302	SA	9.7	294
	M2	9.0	129	M2	11.3	137
	S2	2.4	77	S2	2.9	84
	N2	2.4	81	N2	2.9	87
	K2	0.6	59	K2	0.8	64
	K1	0.4	63	K1	0.3	152
	O1	1.4	299	O1	2.0	299

Detailed water level variations for specific time periods available on the same web-site both for these two stations and interpolated to a position outside Lillesand show general similarity between all three locations. The Lillesand locations are more similar to Tregde than to Helgeroa. Linear regression

between Lillesand and Tregde gives a regression coefficient of 0.83. The model consequently is set up to use the tidal coefficients for Tregde listed in the table above, adjusted with a factor of 0.83.

### 6.3.2 Hydrochemical conditions on outer boundary

The enclosed fjords are not only transition areas for mixing and transport of freshwater out to the coastal water, but also exchange water with the open coastal waters outside by currents driven by density differences, water level variations and wind. The conditions within the fjords are thus determined by a combined influence from the coastal areas outside and the effects of runoff from land on salinity, temperature and nutrient conditions. This is also simulated in the model.

The model requires a continuous time series description of how temperature, salinity, oxygen and biochemical components vary on the outer boundary. The purpose of the outer boundary input data is to provide varying conditions outside the model area to get realistic effects of water exchange driven by variations in water level and stratification outside the fjord areas.

For this purpose, the data from the national coastal monitoring have been used (Moy et al. 2005). Data from the upstream stations outside Arendal (St. 2 and St. 3) have been used to create a table describing the seasonal variation as average and standard deviation by month and depth. Data from depths 0, 5, 10, 20 and 30 m are used, covering the depth range of the limiting transport cross sections between fjord regions and the open coast. The following variables are used:

- Temperature, salinity, oxygen
- Inorganic nutrients nitrate (+nitrite), orthophosphate and silicate.
- Total nitrogen and phosphorus
- Particulate organic carbon, nitrogen and phosphorus

The resulting monthly table of means and standard deviations is included in Appendix A. It shows that total P in the coastal water is about 0.8  $\mu\text{M}$  (25  $\mu\text{g P/l}$ ) in winter and 0.35-0.40  $\mu\text{M}$  in summer, fairly homogeneous over the upper 30 m. The inorganic orthophosphate fraction makes up about 60 to 70 % of the total in winter, and in summer about 10 % in the upper 5 meter, increasing to about 30 % at 30 m depth. The residual difference TotP-PO<sub>4</sub>P-POP, which may be bacterial phosphorus, is on average about 0.15  $\mu\text{M}$ , or about 4.5  $\mu\text{g P/l}$ , for all depths and months.

Nitrogen is measured as total N, inorganic nitrate+nitrite, ammonium and particulate organic N. Total N varies from around 20  $\mu\text{M}$  (280  $\mu\text{g/l}$ ) in winter to around 15  $\mu\text{M}$  in summer as average over the upper 30 meter, with decreasing values with depth at all seasons. The nitrate fraction is a minor part of the total, 30 to 40 % in winter and only 1 to 2 % in summer, so the relative depletion of inorganic N is larger than for phosphorus. Ammonium is more constant through the year, varying around 0.5 to 1.5  $\mu\text{M}$ . The residual N not accounted for by inorganic or particulate organic N is also more or less constant, with averages around 10  $\mu\text{M}$  for all seasons and depths.

For silicate, only the dissolved inorganic concentration is measured. It varies from about 7-8  $\mu\text{M}$  (200  $\mu\text{g Si/l}$ ) in winter to 0.5-2  $\mu\text{M}$  in summer.

Particulate matter is found in highest concentrations close to the surface through the year, with carbon concentrations in the surface varying from 10  $\mu\text{M}$  (120  $\mu\text{g C/l}$ ) in winter to about 20  $\mu\text{M}$  from May to October, nitrogen in C:N proportions 7:1 and C:P about 100:1 (atomic ratios).

Input to the model is created as time series based on this table (Appendix A), with irregular variation around the average seasonal curve at each depth. The variation is created by an advanced random number generator creating series with a specified dominating frequency and with standard deviation as specified in the table. These time series thus have the same general seasonal patterns and short-term varying character as observed, but do not constitute historical time series.

The physical variables and the inorganic nutrient concentrations are used directly, while the total and particulate concentrations of C, N and P are distributed on the active components in the model by assuming similarity with distribution within the model. This is a way of making simulations more realistic, because phytoplankton and other biomasses will then be contained in the water entering the fjord basins from the outer boundary in the model simulations, as it is in reality, while avoiding modelling the processes in the outer boundary.

Concentrations of particulate C, N and P are distributed on phytoplankton, zooplankton and dead organic matter in the same proportions as within the model, using an area-weighted average over basins at each depth.

Total N and P often exceeds the sum of the other measured components, for N even after subtracting an assumed inactive fraction of 100 µg N/l dissolved organic N (humic substances). The N and P that is thus not accounted for, is assumed to represent bacterial biomass (nano-plankton) that is not filtered as particulate matter, and this is used to set the bacterial concentration in the water flowing in from the outer boundary, within bounds set by fixed C:N:P ratios.

Silicium in diatoms is set in proportion to the carbon concentration by assuming the same C:Si ratio in diatoms as within the model. This comes in addition to the dissolved silicate that is measured in the coastal monitoring.

### **6.3.3 Meteorological input data**

The model also uses a detailed timeseries for meteorological data as input data to describe effects of wind, precipitation, humidity and clouds on exchange of heat, oxygen, water and light radiation for phytoplankton growth. Meteorological data from Oksøy Lighthouse (station no. 39100) have been acquired from the online service of the Norwegian Meteorological Institute (met.no) at URL [www.eklima.no](http://www.eklima.no). Data for the 10-year period from 1994 to 2003 have been used. The data series has observation 4 times per day, at hours 0, 6, 12 and 18 (UTC), including the required variables.

### **6.3.4 Ordinary runoff to the fjord areas**

#### **Available data – distribution on components**

The model requires monthly data for input of water and important physical and biochemical components, more specifically:

- water volume
- total phosphorus
- total nitrogen
- dissolved silicate
- total organic carbon
- temperature
- minimum amount of particulate carbon
- maximum limit for ammonium fraction of total N

From TEOTIL, discharges of water, total N and P has been calculated for 7 REGINE areas with monthly resolution. Data for normal runoff are set up based on these calculations, given as monthly values of water flow, total N and P.

The specified concentrations are distributed on particulate matter and dissolved nutrients by using constant distribution factors.

Total carbon in the runoff is assumed to be 5 times higher than nitrogen. Nitrogen is distributed with 70 % as nitrate and 30 % in organic matter, and for phosphorus with at most 80 % bound in organic matter, but within 1 % of organic carbon.

Very little data are available for silicate concentration in runoff, but in the model generally a seasonal concentration curve has been used, varying from 3 mg SiO<sub>2</sub> per litre in winter to 2 mg/l in summer, based on earlier data from rivers Glomma and Dramselva (see Bjerkeng 1994a). There are no measurements of silicate neither in the runoff to these fjords or for the fjord water. The seasonal variation have been adopted, however, in the background scenarios finally used, the concentrations were reduced to 50 % in an attempt to get measured particulate carbon, mainly from silicate-dependent diatoms down towards levels indicated by the observations of total particulate matter in the fjord areas.

### Geographical distribution

For Kaldvellfjord, the runoff as calculated by TEOTIL is assigned to the inner, central basin 2, the area from Kaldvell to Helldal, and will in the model simulations mix into the other basins with water transports. For Valleverdfjord, the TEOTIL runoff is specified separately for the eastern and western part of the catchment. The eastern part roughly corresponds to model basins 1-6, and the western part to model basins 9 and 10 as shown in **Figure 7**. The proportion is more or less the same for water, P and N, and over the months, with 58 % going to the eastern part. In the model, the total runoff is implemented as one source, but it is apportioned to the fjord basins as shown in **Table 8**, roughly based on the size and locations of sub-catchment. For Isefjærfjord, the runoff is similarly distributed on the model basins.

**Table 8.** Distribution of ordinary runoff to model basins in Vallesverdfjord

Main part of catchment	Model basin	% of total runoff
East	1	2
	2	3
	3	5
	4	10
	5	5
	6	35
West	7	10
	9	15
	10	5
	11	10
SUM		100

**Table 9.** Distribution of ordinary runoff to model basins in Vallesverdfjord

Model basin	% of total runoff
1	5
2	30
3	30
4	7
5	7
6	7
7	7
8	7
SUM	100

### Creating time series from seasonal input table

Time series for runoff are created in the model by a combination of interpolation between monthly averages and random variations around the interpolated values. The variational pattern is based on daily runoff data from 1990-2006 from the nearby NVE measuring station (Kilåi), with a catchment area of 64 km<sup>2</sup>, of the same size as the catchment areas to the model fjords. The residuals in  $\ln(\text{Waterflow})$  around a seasonal model based on Fourier terms with 1 and 2 periods per year has a standard variation varying from 0.75-1.0 in winter to 1.4-1.7 in the summer months (June-September). The autocorrelation function of the short-term variations indicate an effective response time of 15 days for the random variations (the interval for which the autocorrelation is approximately  $\exp(-1)=0.36$ ), this is used as the basis for selecting a response frequency of 0.067 (inverse response time) for the runoff random variations simulated in the model:

$$Q(t) = Q_{avg}(t) \cdot \exp(R(t)),$$

where  $R(t)$  is the random variation, implemented as first order Ornstein Uhlenbeck series with 15 days response time. The random series are propagated through time in small time-steps independent of the variable model time-steps so that repeated runs using the same random seed creates exactly the same series, for better comparison of scenarios.

### 6.3.5 Nitrogen runoff from explosives used in road construction

Blasting of 16.9 mill. tons (7.7 mill m<sup>3</sup>) of rock by use of 0.65 or 2.5 kg explosives per m<sup>3</sup> rock for earth works and tunnel works, respectively, results in a potential runoff of 900 tons of nitrogen. About 500 tons of N may enter the more or less landlocked fjords Kaldvellfjord, Vallesverdfjord and Isefjærfjord in the Lillesand-Kristiansand area. This is if all used nitrogen is leached to these fjords. For this calculation we also assumed 80% of NH<sub>4</sub>NO<sub>3</sub> in the explosives.

Only a minor amount of N from explosives will probably be dissolved in water and leached, 10-15% has been indicated. The rest will be oxidized to N-oxides by blasting and driven off to the atmosphere. An unknown amount may be re-deposited by precipitation, so the exact percentage is not known. Here, we therefor choose to use the potential leaching as a worst-case scenario, i.e. 100% leaching, and come back to this issue in the discussion.

The scenario for N run-off from the road construction to the three fjords that are used as input data in the simulations with the fjord model has been set up according to **Table 10**, showing which road segments have runoff to different fjord basins.

The potential accumulation of nitrogen from explosives over time according to the mass calculations on the progress schedule for the road project is shown in **Figure 9**. As the plot shows, the work started in late summer 2006. The vertical axis is placed at date 2007-03-31, just after the last available monitoring data. At that time the work had progressed to a stage where 30-40 % of the total projected amount had been accumulated in the Kaldvellfjord east and Vallesverdfjord west catchments, 8 % for Vallesverd east, and 3-4 % for Kaldvellfjord west and Isefjærfjord. Except for Vallesverdfjord east, most of the N accumulation will be realised by mid-summer 2008.

**Table 10.** Overview of potential nitrogen release – link between road sections/deposits and fjord basins.

Fjord	Basin	Main road section	Road segment (m)	Deposit description	Total runoff (ton N)
Kaldvellfjord	Eastern basin: Kilen-Kaldvell	2	9000-11250	M13 Bådestø	42.6
	Western basin: Kaldvell - Helldal - Dypvik		11500-13500	M14 Sea Deposit M15 Stordalen M16 Gaupemyr	134.0
Vallesverdfjord	Eastern basin	4	21250-25000	M17 Mannfalldalen M18 Langemyr M19 Gåsedalen	207.5
	Western basin		25250-28500	M20 Gale Raundalen	128.9
Isefjærfjord	Inner basin	5	28750-30500	M21 Studedalen	25.6

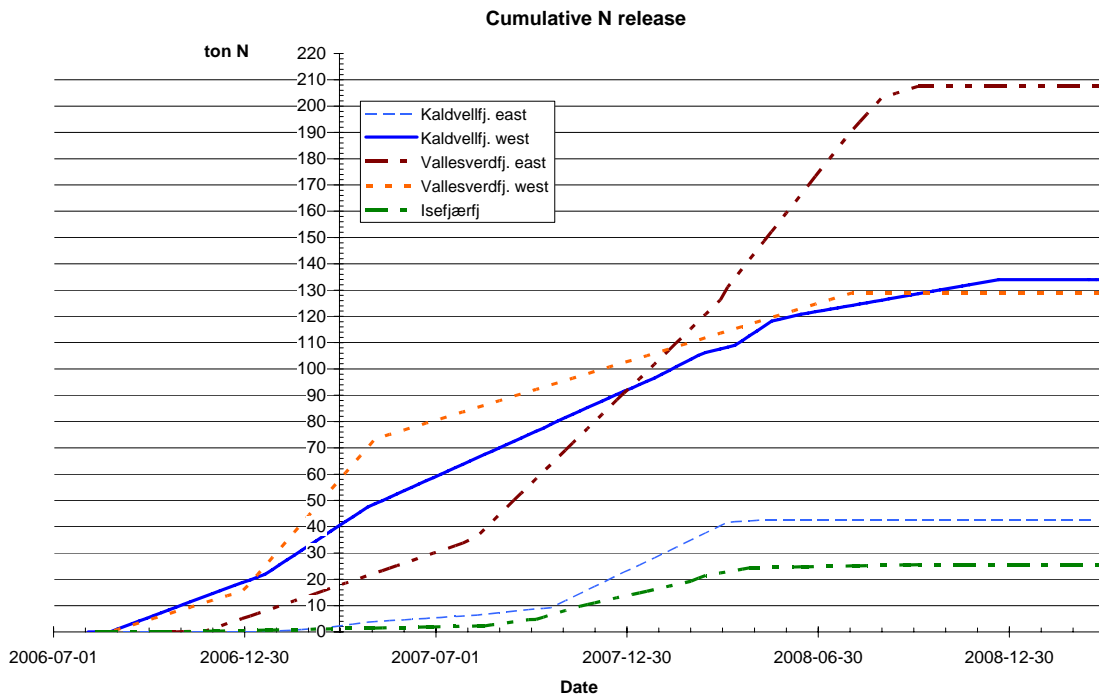


**Figure 9.** Projected potential N-release from the road construction, as cumulative amount of N for the main fjord regions.

For the model runs, the N-leakage to the fjord regions is specified by a combination of buildup of accumulated N and release of N by leakage from the accumulated amounts. The accumulated production of N in each catchment is specified by a sequence of values  $(t_i, M_i)$ , with  $t_i$  = point in time and  $M_i$  =cumulative amount of N  $i=0, n$  with  $t_0=0$  as the starting point for which  $M_0=0$ . The sequences basically are lists of the breakpoints in the curves in **Figure 9**, the details are shown in **Table 11**.

The accumulation and leakage of nitrogen is modelled in a very simple manner by assuming a constant specific rate of release  $r$  for the remaining accumulated amount of nitrogen at any time. During each interval  $(i, i+1)$ , the rate of change for net remaining amount of released nitrogen ( $A$ ) is given by:

$$\frac{dA(t)}{dt} = \frac{M_{i+1} - M_i}{t_{i+1} - t_i} - r \cdot A(t)$$

The second term in the differential equation is the release of N to the fjord basin. The equation has a stepwise analytical solution:

$$A(t) = A_{eq,i} + (A(t_i) - A_{eq,i}) e^{-r(t-t_i)} \quad t_i < t \leq t_{i+1} \quad \text{with} \quad A_{eq,i} = \frac{M_{i+1} - M_i}{r(t_{i+1} - t_i)}$$

where  $A_{eq,i}$  is the equilibrium amount of nitrogen in interval  $(i, i+1)$  as a balance between production and release in the interval  $(i, i+1)$ . The actual amount will approach the equilibrium asymptotically in each interval.

In the model runs, it is assumed that the released nitrate occurs as bioavailable nitrate.

**Table 11.** Sequences of breakpoints in cumulative nitrogen release curves for the main regions relating to the modelled fjords.

Area	Date	Days from 2006-01-01	Cumulative production of nitrogen from explosives $M_i$ (tons)
<b>Kaldvellfjord east</b>	2007-01-26	391	0.00
	2007-03-23	447	1.42
	2007-05-04	489	3.71
	2007-08-17	594	6.38
	2007-10-26	664	9.13
	2008-04-12	833	41.69
	2008-05-17	868	42.58
<b>Kaldvellfjord west</b>	2006-08-24	236	0.00
	2007-01-19	384	21.88
	2007-04-27	482	47.45
	2008-05-17	868	118.18
	2008-12-20	1085	133.95
<b>Vallesverdfjord east</b>	2006-10-26	299	0.00
	2006-11-23	327	0.24
	2007-07-27	573	33.72
	2007-08-10	587	36.44
	2008-03-22	812	123.54
	2008-08-02	945	190.88
	2008-08-30	973	203.06
	2008-10-04	1008	207.51
<b>Vallesverdfjord west</b>	2006-08-24	236	0.00
	2006-12-28	362	15.39
	2007-05-04	489	73.37
	2008-08-02	945	128.95
<b>Isefjærfjord</b>	2006-10-26	299	0.00
	2007-08-17	594	2.27
	2007-09-28	636	4.68
	2007-10-12	650	5.57
	2007-11-16	685	9.76
	2008-03-01	791	19.29
	2008-03-15	805	21.42
	2008-04-26	847	24.33
	2008-10-04	1008	25.57

#### 6.4 Scenarios with N from the road construction – comparison with background scenarios.

Background scenarios with ordinary runoff were simulated for all three fjords over 5 years, with different sets of coefficients to get realistic stratification and concentrations compared to available observations. Some results are shown in Appendix B. Salinity and temperature stratification is about as observed, and surface nitrates varies from low values in summer to about 200  $\mu\text{gN/l}$  in winter as time series plots for nitrate in different model depths. Results for temperature, salinity, oxygen, orthophosphate and silicate are shown and discussed in Appendix B. The simulations start from initial conditions established by spin-up runs with the model.



**Figure 10** to **Figure 13** show results of model simulations as sequences of comparison time series plots for selected basins. For Kaldvellfjord, results are shown for basin 2, the inner southwestern basin which receives the largest N input. For Vallesverdfjord, results are shown for basin 6 and 10, the two inner basins that will receive N from the road construction. For Isefjærfjord, results are for the innermost basin (2), which is the recipient of N from the road.

Each sequence includes three plots, with time series for concentrations of respectively nitrate (NO<sub>3</sub>N), particulate N (PARTN) and particulate C (PARTC). Most of the particulate matter is phytoplankton. The concentrations are averages for the surface layer down to approximately 1 m depth. Nitrate and particulate N are shown as µg N/l and particulate C as µg C/l.

Each plot compares the results of two parallel runs, xxxx\_A02 with only ordinary runoff, and xxxx\_B with nitrogen from the E18 project as additional leaking to the surface layers of the fjord areas (xxxx = abbreviation for fjord area). Run B has otherwise exactly the same model specifications and input data time series as the corresponding A02 simulation.

According to these results, the E18 road project may be expected to potentially increase nitrate concentrations in the surface layers of the inner basins by a factor of 2 over a period of 2 years. In Kaldvellfjord (**Figure 10**) this leads to very little noticeable change in amount or composition of particulate matter. In Vallesverdfjord, (**Figure 11** and **Figure 12**) increases of peak values of organic N with up to 100 % occur, and at the same time increases of at most 30 % in particulate C compared to the background scenario. However, the change occurs only during limited time intervals, and is not accompanied by any noticeable effect on oxygen contents below the surface layer. In Isefjærfjord there is a more prolonged increase towards the end of period with increased nitrate, also with a smaller increase in C; there are small changes in oxygen conditions during some periods, but in general very little change from the background scenario to the scenario with N input from the road construction.

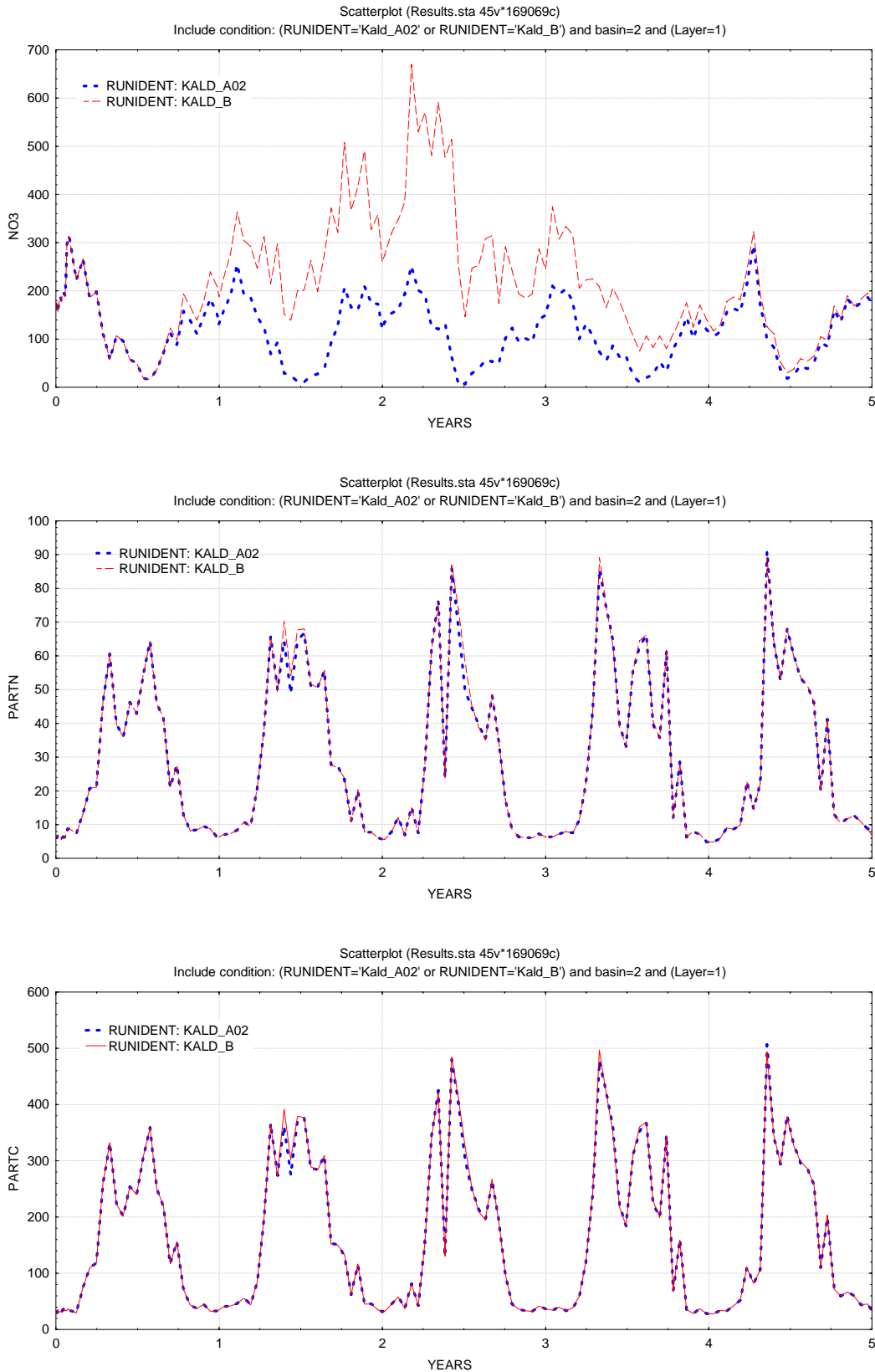


**Figure 10.** Simulated nitrate (NO<sub>3</sub>-N as  $\mu\text{g N/l}$ ), particulate N (PARTN as  $\mu\text{g N/l}$ ) and particulate C (PARTC as  $\mu\text{g C/l}$ ) in the surface layer of the Kaldvellfjorden basin 2 for ordinary runoff (A02) and with N from the E18 road construction.

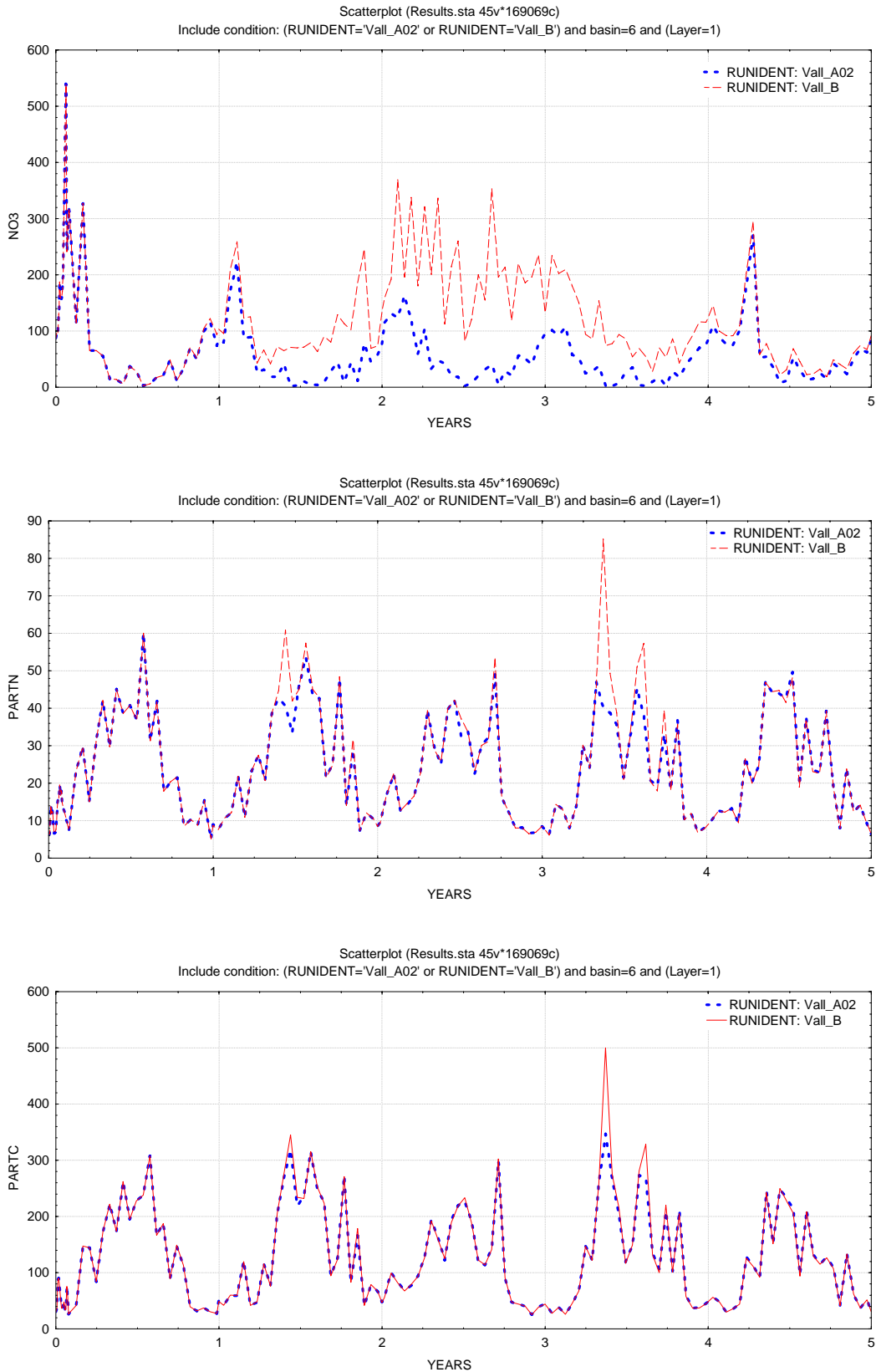


**Figure 11.** Simulated nitrate (NO<sub>3</sub>-N as µg N/l), particulate N (PARTN as µg N/l) and particulate C (PARTC as µg C/l) in the surface layer of the Vallesverdfjorden basin 6 for ordinary runoff (A02) and with N from the E18 road construction.

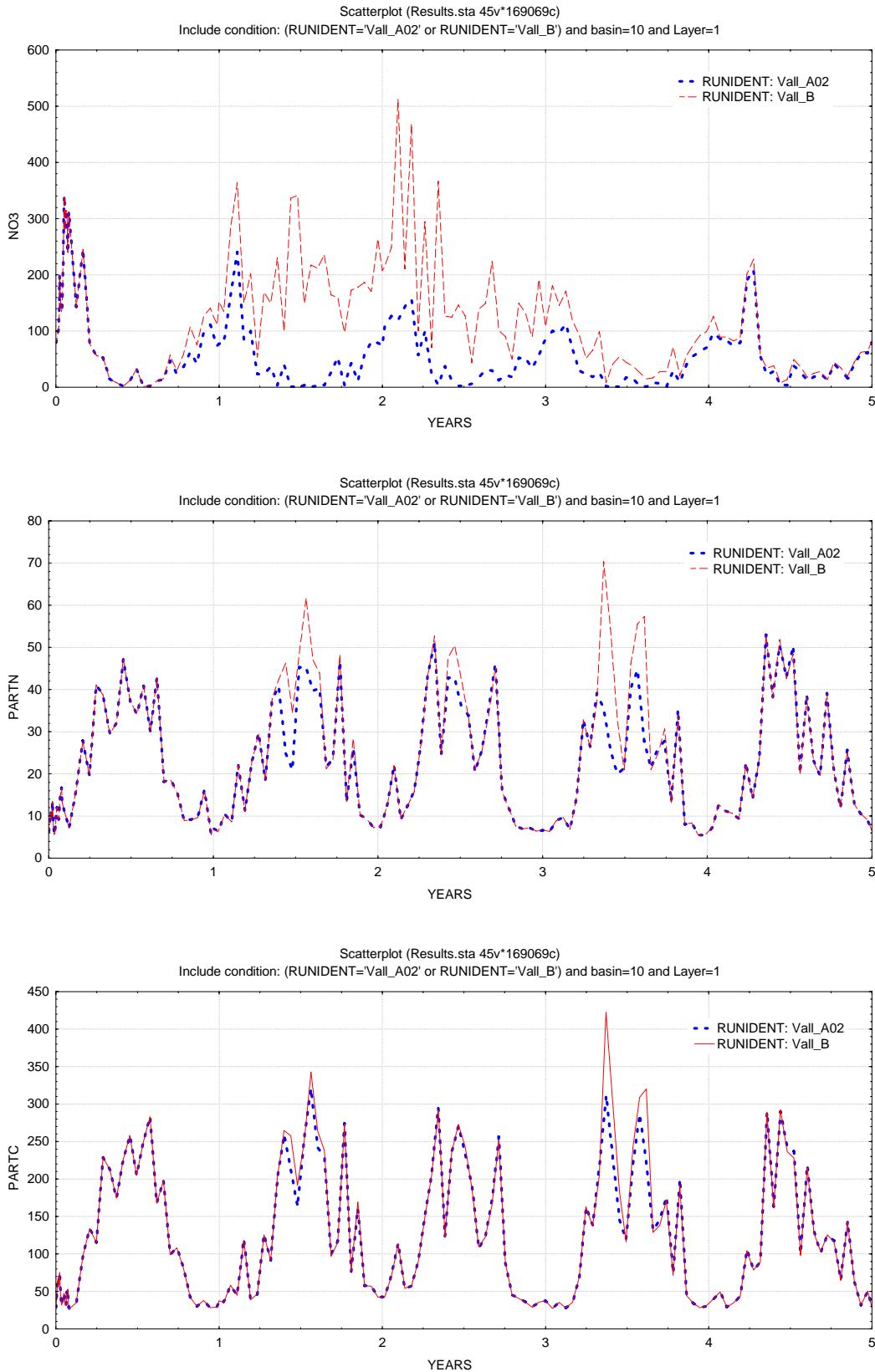


**Figure 12.** Simulated nitrate (NO<sub>3</sub>N as µg N/l), particulate N (PARTN as µg N/l) and particulate C (PARTC as µg C/l) in the surface layer of the Vallesverdfjorden basin 10 for ordinary runoff (A02) and with N from the E18 road construction.

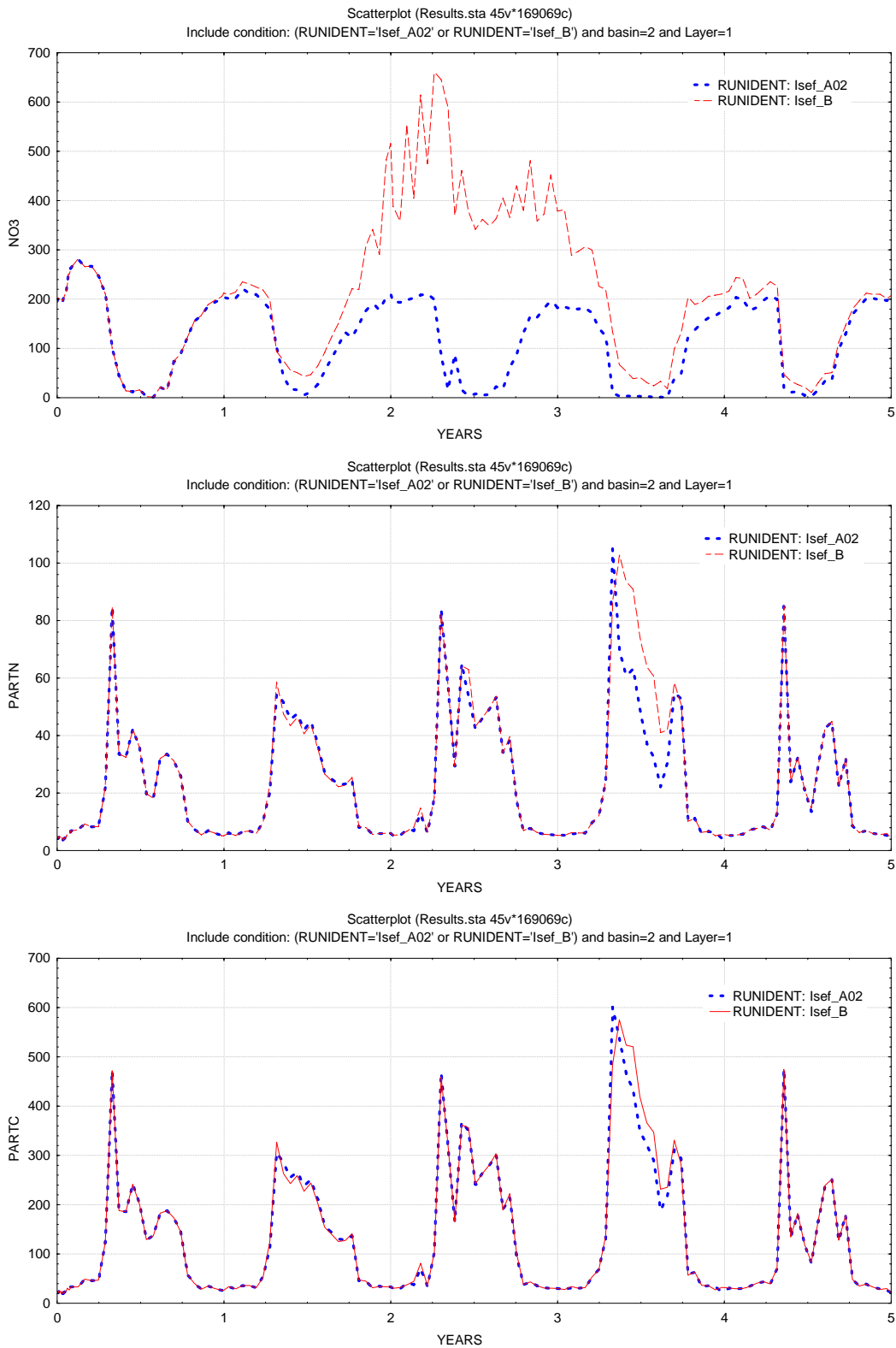


**Figure 13.** Simulated nitrate (NO<sub>3</sub>N as µg N/l), particulate N (PARTN as µg N/l) and particulate C (PARTC as µg C/l) in the surface layer of the Isefjær fjorden basin 2 for ordinary runoff (A02) and with N from the E18 road construction.

## 7. Discussion

We have estimated the N load to several fjords along the E18 Grimstad-Kristiansand road construction area. The natural and local, man-made contributions have been compared with the potential added load of about 900 tons of N from explosives used at the construction site. The potential N load from explosives was estimated to be 3-5 times the annual background load for Kaldvellfjorden and Isefjærfjorden, but as high as 15-16 times for Vallesverdfjorden.

The resulting potential increases in N concentrations (i.e. nitrate concentrations) are significant for all fjords. In the central basin of Kaldvellfjorden and in the innermost basins of the two other fjords more than a doubling may occur for a 2-3 years period. The ordinary summer-minimum, with an almost total loss of nitrate from the surface layers, may be replaced by relatively high concentrations in this season.

The reason for the small modelled effects in fjords of the potential nitrate addition is apparently that the algae production is limited by access to phosphate. And with efficient grazing of phytoplankton, keeping the growth-rate high, the excess nitrogen cannot be used for increased production of biomass.

The growth of phytoplankton is controlled by the supply of nutrients. All algae needs N and P and in addition diatoms need silicate. A balanced N/P-ratio in seawater for fast-growing phytoplankton is 16:1 (atomic ratio, corresponding to a weight ratio of 7:1), while the ratio is much higher (often >100) in freshwater. In a fjord with freshwater run-off the surface layer will be a mixture of freshwater and seawater, resulting in an increased N/P-ratio in the mixed upper water layer compared to seawater, where the ratio is closer to N:P balance. In addition the concentration of P is lower in freshwater than in seawater. This leads to lack of P during algal growth in freshwater-influenced surface water in the sea. Large supplies of bio-available N to water masses where phytoplankton growth is limited by P will not increase the primary production.

A high N/P-ratio may affect the phytoplankton composition. Experiments have shown that increase of the N/P-ratio disfavors the diatoms while slow-growing algal groups like dinoflagellates including potential toxin producing species are favored caused by high P-uptake efficiency.

To avoid increased biomass of such algae in water with high N/P-ratio, presence of zooplankton grazing on these algae is necessary. If those grazers are absent, the phytoplankton will bloom, enter a phase with low growth rate, die, and sink to the bottom for consumption by bottom-living animals or decomposition by use of oxygen leading to oxygen depletion in the bottom water. If the phytoplankton is efficiently limited by grazing pressure from zooplankton, this will keep the biomass concentrations at reasonably low levels and sustain a high growth rate of phytoplankton through remineralisation of nutrients which is reused by phytoplankton. Adding excess nutrients that are not limiting in such a situation will not result in extra uptake of this nutrient, and will thus not lead to increased biomass. This seems to be the case for the fjords along the E18, as shown by the model simulations. There is some effect on the surface layer as increased particulate matter, and in periods a decrease in particulate C:N ratios, but this does not seem to lead to a change from fast-growing, grazed phytoplankton to a situation with algal blooms.

The model results are not accurate, and there are indications that the model gives larger particulate biomass than observed (based on total suspended matter; carbon was not measured), but the differences between the scenarios should still be realistic.

As stated earlier, only a minor amount of the N from explosives will probably be dissolved in water and leached, 10-15% has been indicated, but an unknown amount of the N-oxides after blasting may be deposited again by precipitation, so the exact percentage is not known. The model result is thus a worst case scenario, strongly suggesting that the actual effects will be insignificant.

## 8. Conclusion

The model simulations show that the E18 Grimstad-Kristiansand road construction may be expected to potentially increase nitrate concentrations in some fjord basins by a factor of 2 over a period of 2 years. There is a secondary increase of particulate N, especially towards the end of the impact period, but the effect is mainly a more N-rich biomass; the response in particulate carbon is much smaller. For oxygen levels at depth, the model does not predict any noticeable change. Further, the actual N-leaching will be significantly less than the potential, strongly suggesting minor changes.

The reason for the small effects is apparently that the algae production is limited by access to phosphate, so that excess N can not be used for increased production. Also, algae grazing by zooplankton and N-accumulation in the algal biomass may contribute to a smaller ecological effect than suggested by the nitrate increase. The released amount of N from explosives thus appears to be transported in diluted concentrations into the coastal current, rather than having effects in the enclosed fjords.

## 9. References

- Bjerkeng, B., 1994a. Eutrofimodell for indre Oslofjord. 1: Praktisk utprøving på indre Oslofjord. NIVA-rapport 3112. 96 s.
- Bjerkeng, B., 1994b. Eutrofimodell for indre Oslofjord. 2: Faglig beskrivelse av innholdet i modellen. NIVA-rapport 3113. 134 s.
- Kroglund, T., Molvær, J. og Moy, F. 2007. Kjemisk og biologisk tilstand i fjorder før bygging av ny E18 Grimstad-Kristiansand. NIVA-rapport 5348. 72 s.
- Moy, F., Aure, J., Dahl, E., Falkenhaus, T., Green, N., Johnsen, T., Lømsland, E., Magnusson, J., Pedersen, A., Rygg, B., Walday, M. 2005. Langtidsovervåking av miljøkvaliteten i kystområdene av Norge. Kystovervåkingsprogrammet. Årsrapport for 2005. NIVA-rapport 5286. 94 s.
- Selvik, J.R, Tjomsland, T., Borgvang, S.-A. og Eggestad, H.O. 2005. Tilførsler av næringssalter til Norges kystområder, beregnet med tilførselsmodellen TEOTIL. Statlig program for forurensningsovervåking, Rapport nr 943/2005, TA-2137/2005. NIVA-rapport 5103. 57 s.
- Tjomsland, T. og Bratli, J.L. 1996. Brukerveiledning og dokumentasjon for TEOTIL. Modell for teoretisk beregning av fosfor- og nitrogentilførsler i Norge. NIVA-rapport 3426. 84 s.

## Appendix A. Hydrochemical boundary conditions - monthly statistics

Month	Temp		Salinity		Oxygen		TotP		PO4P		TotN		NO3N		NH4N		SiO3		POC		PON		POP		
	Mean	Stdv	Mean	Stdv	Mean	Stdv	Mean	Stdv	Mean	Stdv	Mean	Stdv	Mean	Stdv	Mean	Stdv	Mean	Stdv	Mean	Stdv	Mean	Stdv	Mean	Stdv	Mean
1 0	3.76	1.78	30.08	2.09	7.51	0.39	0.82	0.17	0.54	0.13	22.66	4.92	8.09	2.26	1.21	0.55	7.53	2.25	9.61	4.24	1.36	0.67	0.089	0.070	
1 5	4.05	1.64	30.48	1.98	7.42	0.39	0.81	0.15	0.58	0.09	20.13	3.48	8.15	2.14	0.82	0.41	7.22	1.59	6.87	2.48	0.90	0.31	0.072	0.042	
1 10	4.48	1.57	31.15	1.82	7.28	0.38	0.80	0.13	0.59	0.10	19.51	2.74	8.13	2.09	0.90	0.56	6.95	1.44	6.35	2.02	0.87	0.30	0.069	0.038	
1 20	5.37	1.38	32.33	1.50	7.04	0.36	0.81	0.15	0.60	0.10	18.70	3.73	7.90	2.09	0.66	0.43	6.27	1.43	6.16	2.56	0.82	0.29	0.062	0.035	
1 30	6.00	1.14	33.09	0.89	6.84	0.30	0.78	0.14	0.59	0.09	18.35	3.93	7.54	1.76	0.60	0.50	5.72	1.14	5.86	2.77	0.82	0.43	0.060	0.039	
2 0	3.23	1.85	29.84	3.16	7.66	0.62	0.81	0.13	0.55	0.10	22.53	4.76	8.29	2.91	0.96	0.66	7.82	3.25	10.00	5.36	1.51	1.07	0.083	0.059	
2 5	3.42	1.72	30.43	2.79	7.56	0.57	0.82	0.10	0.58	0.09	19.62	2.98	8.36	2.93	0.73	0.45	7.23	2.77	8.17	5.35	1.21	1.04	0.076	0.057	
2 10	3.85	1.52	31.30	2.07	7.39	0.40	0.83	0.10	0.59	0.10	19.70	4.22	8.46	2.69	0.73	0.49	6.96	2.49	7.32	2.96	1.05	0.56	0.070	0.039	
2 20	4.64	1.41	32.65	1.34	7.15	0.39	0.81	0.09	0.61	0.09	18.37	2.83	8.55	2.12	0.68	0.48	6.25	1.82	6.94	4.02	0.98	0.72	0.060	0.037	
2 30	5.22	1.35	33.35	1.13	7.05	0.39	0.80	0.08	0.60	0.08	18.32	3.07	8.24	1.90	0.64	0.43	5.73	1.52	7.12	4.52	0.96	0.66	0.048	0.025	
3 0	2.95	1.40	28.91	2.66	8.14	0.71	0.63	0.13	0.25	0.17	19.46	3.88	4.48	4.55	1.07	0.85	3.16	3.14	18.32	11.18	2.72	1.50	0.192	0.106	
3 5	3.04	1.39	29.66	2.39	8.08	0.76	0.64	0.14	0.28	0.19	18.67	4.03	4.91	4.70	0.67	0.41	3.09	3.15	15.73	9.21	2.58	1.60	0.192	0.118	
3 10	3.36	1.26	30.75	2.06	7.80	0.53	0.64	0.14	0.32	0.18	17.70	4.18	5.65	4.37	0.62	0.34	3.11	2.94	13.90	8.52	2.27	1.65	0.173	0.104	
3 20	3.99	1.07	32.11	1.68	7.47	0.39	0.69	0.11	0.41	0.16	18.19	4.38	6.84	4.15	0.71	0.39	3.52	2.65	10.81	5.68	1.81	1.17	0.142	0.089	
3 30	4.70	0.85	33.30	0.89	7.17	0.30	0.76	0.09	0.52	0.11	18.26	4.01	8.46	3.50	0.77	0.51	4.42	2.07	9.55	5.38	1.38	0.85	0.098	0.055	
4 0	4.99	1.20	26.20	4.24	7.85	0.33	0.45	0.13	0.13	0.09	19.62	5.00	2.95	3.84	1.33	0.78	2.01	2.52	14.90	7.21	2.23	1.17	0.132	0.061	
4 5	4.86	1.05	27.16	3.73	7.82	0.31	0.41	0.13	0.12	0.11	16.76	3.90	3.04	3.94	0.98	0.55	1.49	1.22	11.66	5.47	1.85	0.84	0.132	0.059	
4 10	4.69	0.98	29.21	3.02	7.72	0.36	0.43	0.12	0.16	0.12	16.29	3.77	3.36	3.78	1.02	0.45	1.33	1.12	10.22	5.65	1.54	0.76	0.106	0.058	
4 20	4.77	0.72	32.13	1.45	7.43	0.43	0.53	0.15	0.29	0.16	17.57	5.09	5.64	4.80	1.23	0.52	1.80	1.45	8.76	4.88	1.26	0.73	0.083	0.054	
4 30	5.01	0.64	33.33	0.96	7.14	0.48	0.61	0.16	0.43	0.18	17.58	4.32	7.10	4.21	1.24	0.60	2.56	1.66	7.73	4.18	1.08	0.58	0.072	0.053	



Month	Temp		Salinity		Oxygen		TotP		PO4P		TotN		NO3N		NH4N		SiO3		POC		PON		POP		
	Depth	Mean	Stdv	Mean	Stdv	Mean	Stdv	Mean	Stdv	Mean	Stdv	Mean	Stdv	Mean	Stdv	Mean	Stdv	Mean	Stdv	Mean	Stdv	Mean	Stdv	Mean	Stdv
		°C	ml/l	µM	µM	µM	µM	µM	µM	µM	µM	µM	µM	µM	µM	µM	µM	µM	µM	µM	µM	µM	µM	µM	µM
5	0	9.89	2.21	23.67	3.93	7.30	0.31	0.48	0.23	0.06	0.09	21.85	6.57	1.15	1.62	1.20	0.70	2.13	1.97	20.01	6.42	2.92	0.96	0.164	0.062
5	5	9.28	1.88	24.95	3.56	7.39	0.32	0.42	0.18	0.05	0.08	17.28	2.75	1.06	1.53	0.72	0.54	1.53	1.29	16.97	5.64	2.49	0.92	0.168	0.059
5	10	8.01	1.67	27.83	3.37	7.35	0.41	0.43	0.19	0.09	0.13	17.56	3.37	2.00	2.34	0.87	0.48	1.24	0.94	15.87	6.66	2.39	1.12	0.163	0.060
5	20	6.50	1.07	32.04	1.53	7.18	0.37	0.49	0.21	0.21	0.19	17.19	3.13	4.22	2.81	1.50	0.74	1.42	1.12	9.27	3.87	1.40	0.71	0.094	0.048
5	30	6.19	0.89	33.28	0.93	6.97	0.27	0.52	0.20	0.32	0.17	16.64	3.40	4.75	2.54	1.59	0.70	1.85	1.10	7.78	3.38	1.10	0.49	0.061	0.027
6	0	13.22	1.83	26.09	3.87	6.79	0.46	0.42	0.16	0.05	0.05	18.14	3.39	0.86	1.64	0.72	0.60	0.89	0.81	20.97	6.30	2.83	0.97	0.165	0.047
6	5	12.42	2.09	27.59	3.74	6.86	0.58	0.41	0.10	0.05	0.05	16.79	3.02	1.03	1.95	0.63	0.67	0.70	0.60	19.29	5.05	2.73	1.21	0.183	0.051
6	10	11.00	2.17	30.07	3.15	6.77	0.69	0.42	0.09	0.06	0.04	17.29	3.51	1.81	2.36	0.99	0.94	0.81	0.52	17.95	6.38	2.59	1.13	0.183	0.058
6	20	9.23	1.69	32.78	1.07	6.50	0.63	0.46	0.12	0.15	0.08	16.77	3.78	2.42	2.17	1.70	0.95	1.38	0.64	11.99	5.82	1.87	1.17	0.129	0.057
6	30	8.40	1.37	33.68	0.74	6.46	0.59	0.51	0.17	0.23	0.10	15.74	3.07	2.39	1.60	2.03	0.98	1.78	0.77	9.70	5.14	1.46	0.99	0.098	0.071
7	0	16.33	1.76	27.40	2.98	6.13	0.26	0.34	0.11	0.04	0.03	17.33	4.17	0.36	0.69	0.85	1.06	0.56	0.33	19.07	9.80	2.40	0.98	0.126	0.055
7	5	15.88	1.63	28.50	2.53	6.15	0.31	0.35	0.09	0.04	0.03	15.68	2.73	0.38	0.79	0.59	0.67	0.54	0.35	18.04	9.54	2.29	1.05	0.136	0.052
7	10	14.77	1.53	30.28	1.66	6.09	0.38	0.37	0.09	0.05	0.03	15.55	2.89	0.54	0.89	0.61	0.58	0.66	0.50	16.93	6.72	2.23	0.86	0.144	0.060
7	20	12.83	1.56	32.60	0.96	5.94	0.43	0.40	0.10	0.10	0.07	14.90	2.99	1.07	1.29	1.10	0.84	1.15	0.67	14.62	6.20	1.89	0.73	0.130	0.051
7	30	11.17	1.60	33.62	0.66	5.88	0.35	0.45	0.12	0.20	0.10	14.86	3.24	1.55	1.34	1.62	0.72	1.91	0.87	10.23	4.84	1.48	0.91	0.086	0.024
8	0	18.08	1.95	26.54	3.24	5.96	0.31	0.40	0.10	0.06	0.04	18.05	5.20	0.16	0.11	0.72	0.55	0.93	0.64	21.27	11.87	2.74	1.00	0.167	0.074
8	5	17.69	1.87	28.63	2.98	5.89	0.33	0.38	0.10	0.05	0.03	14.19	2.07	0.15	0.16	0.41	0.33	0.94	0.58	17.22	6.97	2.33	0.73	0.165	0.066
8	10	16.90	1.38	30.87	1.95	5.74	0.36	0.38	0.09	0.06	0.05	13.52	2.28	0.21	0.23	0.45	0.38	1.10	0.54	15.32	5.12	2.10	0.64	0.149	0.060
8	20	15.35	1.08	32.79	0.96	5.39	0.42	0.38	0.10	0.09	0.06	12.87	2.15	0.55	0.60	0.71	0.52	1.60	0.60	13.29	5.13	1.78	0.62	0.125	0.045
8	30	13.73	1.73	33.58	0.67	5.35	0.35	0.41	0.09	0.16	0.07	13.69	3.63	1.33	1.37	1.10	0.77	2.27	0.98	10.57	3.92	1.54	0.65	0.093	0.036
9	0	15.89	1.40	28.44	3.11	5.95	0.30	0.45	0.10	0.08	0.05	19.75	5.25	0.26	0.22	0.83	0.54	1.47	0.77	22.66	7.59	2.96	1.07	0.188	0.062
9	5	15.93	1.44	29.01	3.04	5.89	0.34	0.42	0.08	0.07	0.05	14.38	2.33	0.20	0.18	0.48	0.38	1.48	0.79	18.30	8.00	2.33	0.76	0.182	0.068
9	10	15.97	1.43	30.40	2.72	5.70	0.38	0.42	0.18	0.07	0.05	14.47	2.73	0.24	0.24	0.51	0.31	1.47	0.81	16.90	7.90	2.23	0.80	0.162	0.057
9	20	15.74	1.38	32.43	1.60	5.48	0.45	0.38	0.07	0.10	0.06	12.79	1.96	0.47	0.44	0.69	0.45	1.85	1.13	12.64	6.31	1.75	0.83	0.121	0.048
9	30	14.39	1.85	33.56	0.76	5.36	0.53	0.41	0.09	0.17	0.10	12.89	2.19	1.22	1.19	0.84	0.55	2.57	1.24	10.15	4.37	1.41	0.68	0.094	0.044

Month	Depth	Temp °C		Salinity		Oxygen ml/l		TotP µM		PO4P µM		TotN µM		NO3N µM		NH4N µM		SiO3 µM		POC µM		PON µM		POP µM			
		Mean	Stdv	Mean	Stdv	Mean	Stdv	Mean	Stdv	Mean	Stdv	Mean	Stdv	Mean	Stdv	Mean	Stdv	Mean	Stdv	Mean	Stdv	Mean	Stdv	Mean	Stdv	Mean	Stdv
10	0	12.40	1.68	29.21	2.96	6.14	0.40	0.51	0.10	0.16	0.07	16.69	4.42	0.86	0.65	1.21	1.04	2.01	1.02	17.31	11.23	2.50	1.75	0.156	0.078		
10	5	12.59	1.64	29.82	2.82	6.03	0.40	0.49	0.09	0.16	0.08	14.23	3.44	0.78	0.63	0.82	0.62	1.87	0.73	13.43	7.76	1.91	1.11	0.146	0.076		
10	10	12.89	1.57	30.88	2.58	5.88	0.38	0.47	0.09	0.17	0.08	13.70	2.46	0.85	0.67	0.82	0.51	1.91	0.64	11.11	5.75	1.61	0.90	0.122	0.065		
10	20	13.19	1.60	32.50	1.14	5.67	0.32	0.48	0.12	0.21	0.10	12.89	2.23	1.05	0.81	0.91	0.59	2.07	0.65	8.89	5.27	1.37	0.88	0.099	0.061		
10	30	13.13	1.75	33.15	0.98	5.63	0.39	0.48	0.11	0.23	0.12	12.42	2.65	1.31	1.36	0.95	0.83	2.17	0.90	7.95	4.43	1.16	0.75	0.082	0.055		
11	0	8.95	2.09	29.79	2.48	6.57	0.45	0.61	0.12	0.29	0.11	18.45	3.53	2.66	1.43	1.59	1.13	3.61	1.85	13.63	4.74	1.84	0.75	0.109	0.040		
11	5	9.19	2.03	30.56	1.98	6.47	0.42	0.59	0.13	0.31	0.12	15.67	3.12	2.64	1.43	1.19	0.67	3.14	1.41	9.68	4.14	1.38	0.65	0.093	0.032		
11	10	9.66	1.97	31.31	1.71	6.37	0.41	0.58	0.14	0.32	0.13	15.17	2.62	2.66	1.39	1.11	0.65	3.05	1.24	8.10	2.98	1.18	0.49	0.080	0.023		
11	20	10.33	1.77	32.50	1.12	6.10	0.45	0.59	0.15	0.34	0.13	14.85	3.20	2.69	1.29	1.09	0.62	2.79	0.99	7.71	4.94	1.11	0.77	0.066	0.022		
11	30	10.73	1.55	33.25	0.83	5.99	0.42	0.57	0.15	0.35	0.13	14.29	3.11	2.82	1.34	0.92	0.69	2.76	0.86	7.53	4.65	1.04	0.74	0.055	0.022		
12	0	6.75	2.03	29.98	2.35	6.87	0.46	0.68	0.09	0.45	0.09	18.54	3.45	4.90	1.29	1.09	0.55	5.55	2.10	9.02	3.62	1.14	0.61	0.079	0.034		
12	5	7.29	1.83	30.77	2.27	6.77	0.42	0.69	0.10	0.46	0.09	16.94	3.01	4.86	1.23	0.80	0.62	5.05	1.91	7.55	4.29	0.96	0.36	0.068	0.020		
12	10	7.73	1.67	31.45	1.85	6.63	0.37	0.69	0.10	0.47	0.09	16.06	2.11	4.84	1.21	0.72	0.52	4.71	1.78	6.68	1.74	0.90	0.26	0.061	0.015		
12	20	8.39	1.61	32.56	1.47	6.45	0.32	0.67	0.09	0.47	0.09	15.28	1.86	4.80	1.13	0.50	0.42	4.19	1.19	5.90	1.71	0.77	0.25	0.053	0.016		
12	30	8.93	1.37	33.33	0.82	6.32	0.25	0.68	0.11	0.48	0.10	15.06	2.56	4.75	1.20	0.36	0.36	3.94	1.04	6.00	2.72	0.77	0.28	0.047	0.014		

## Appendix B. Simulation results for background scenario

The figures in this appendix show the results of the background scenario for Vallesverdfjord. The figures compare model results for the two inner basins. Basin 6, which is 45 m deep, has open connections to the sea through basin 7, with no sills above 30 m depth, while basin 10, which is 35 m deep, is closed off by a sill at 10 m depth between basin 9 and 10.

The plots include Layers 1, 6, 11 and 16, which for Vallesverdfjord correspond to approximate depths 0.5, 5, 10 and 20 m. Results for basin 10 are shown on the left, and corresponding plots for basin 6 on the right.

The plots show that temperature is more or less homogeneous vertically down to 20 m in Basin 6, due to direct exchange with the coastal waters, while temperature in Basin 10 is more constant at 20 m depth, because the seasonal change depends on vertical mixing of deep water. The same difference is seen between V2 (basin 6) and station V4 (basin 10) in the hydrographical data. Salinity varies in the surface layer in the same range as observed in both basins; the salinity at 20 m depth has less short-term variations in Basin 10 than in basin 6, as is also observed.

Oxygen (ml/l) is quite homogeneous across depths down to 20 m in basin 6, while at 20 m in basin 10 this occurs only in shorter periods in the model results. In the observations lower oxygen values (down towards 3 ml/l) were observed at station V4 at 20 m; but persistent low values were seen in the observations at at 30 m depth at station V4 (Basin 10), while station V6 (basin 2) had about the same oxygen concentrations down to 30 m.

Nitrate in the upper 10 m varies from low values in summer to peaks around 50  $\mu\text{g N/l}$  in winter; this is about the same as in the observations, also for this variable more vertically homogeneous in basin 6 than in basin 10. Orthophosphate peaks at between 20 and 30  $\mu\text{g P/l}$  in winter, generally consistent with the observed winter values for total phosphorus of around 25  $\mu\text{g/l}$  observed from December 2006 to February 2007. Particulate organic carbon has high summer values between 200 and 300  $\mu\text{g C/l}$  in the surface; this is somewhat higher than can be estimated from measured total suspended matter (TSM) in the observations.

